

**Manuscript Title:** Ice injected up to the Tropopause by Deep Convection: 1) in the Austral Convective Tropics **by Dion et al.**

We would like to thank the two referees for the comments that were helpful in improving substantially the presentation and contents of the revised manuscript. We hope we have addressed appropriately all issues raised by the referees.

The referee's comments are repeated in the following paragraphs in black and our responses appear in red. Copy of sentences or paragraphs changed into the paper are repeated and appear in yellow. Sentences or paragraphs deleted into the paper appear crossed-out and in orange. A copy of the entire manuscript with the whole corrections is presented at the end of this report.

## **RESPONSES TO THE ANONYMOUS REFEREE #1**

### **General**

The study presents a detailed investigation of the diurnal cycle of water vapor and especially ice injected by deep convection into the UT and TL of six tropical regions. The region with the highest amount of UT/TL ice and thus probably a major source region for stratospheric water- is identified. For that purpose, a clever data evaluation method was developed combining the satellite observations of MLS (lower geographical and time resolution) and TRMM (higher geographical and time resolution). The method was validated (or better say evaluated, see specific comments) using measurements from the SMILES instrument. The topic of the study is of relevance and suitable for publication in ACP. The manuscript is clearly structured and fluently written, the Figures are also clear and mostly self-explanatory. What I missed in the paper is a more conclusive statement about the importance of the findings and the impact for the research in this area – what new can we learn from this study ? Though the reader can get an idea about this, to my opinion it should be clearly pointed out in the paper at the relevant places (abstract, introduction, conclusions).

We provide some suggestions on that separately below. We also modified the entire introduction (copied at the end of this report) and provide more justification for our work.

A number of specific comments are listed in the following in the order of appearance in the manuscript.

### **Specific comments**

**1) line 9** ‘ The impact of **deep convection** on the water budget ...’

Comment: Isn't it that in this study the magnitude of water and ice in the UT and TL stemming from deep convection is investigated – to estimate the impact on the water budget you would need to know the magnitude of the other sources of ice, yes?

Yes, to be clearer, the sentence l. 9 has been changed to:

~~The impact of deep convection on the water budget from the tropical Upper Troposphere (UT, around 146 hPa) to the Tropopause Level (TL, around 100 hPa) is investigated.~~  
The contribution of deep convection to the amount of water vapor and ice in the Tropical Tropopause Layer (TTL) from the tropical upper troposphere (UT, around 146 hPa) to the

Tropopause Level (TL, around 100 hPa) is investigated. Ice water content (IWC) and water vapour (WV) measured in the UT and the TL by the Microwave Limb Sounder (MLS, Version 4.2) are compared to the precipitation (Prec) measured by the Tropical Rainfall Measurement Mission (TRMM, Version 007).

**2) line 46** ‘.. the region called Maritime Continent (MariCont), the region between the Indian Ocean and the West Pacific ...’

Comment: Figure 4 can be introduced already here – then the reader see better what region is meant.

We surrounded by a red box the MariCont in the Fig.1 and we added this sentence in the caption:

Figure 1: (From top to bottom): (a) (Day+Night)/2 of precipitation measured by TRMM at  $0.25^{\circ} \times 0.25^{\circ}$  resolution (mm/h), (b) (Day+Night)/2 of precipitation at  $2^{\circ} \times 2^{\circ}$  resolution (mm/h), and (c) hour of diurnal maximum of precipitation at  $0.25^{\circ} \times 0.25^{\circ}$  resolution (h in Local Solar Time, LST) in DJF over the period 2004-2017. The red box surrounds the MariCont region.

And added line 199:

... together with the Maritime Continent region (MariCont, the region made of lands and oceans, between the Indian Ocean and the West Pacific, presented by the red box in Fig. 1).

**3) line 120** 2 Datasets Comment: I recommend to rename the section to ‘Instruments’

We renamed the section as you suggested.

**4) line 127** ‘The MLS IWC sensitivity thresholds do not allow to detect low ice content such as cirrus outflow associated with convective events. MLS IWC sensitivity will mostly be able to detect ice from convective cores. Following Livesey et al. (2017), we will not consider IWC measurements less than  $0.02 \text{ mg m}^{-3}$ .’

Comment: All the thin cirrus are missed. How does that impact the results ?

This sentence was not clear enough and have been changed. The detection limit of MariCont ice concentration is  $0.02 \text{ mg/m}^{-3}$  in the TL whatever the origin/source of ice: convective cores or cirrus associated with convective events. Thus, cirrus are not missed.

The new sentence l. 127 is now l.135:

The MLS IWC sensitivity thresholds do not allow to detect low ice content such as cirrus outflow associated with convective events. MLS IWC sensitivity will mostly be able to detect ice from convective cores. Following Livesey et al. (2017), we will not consider IWC measurements less than  $0.02 \text{ mg m}^{-3}$ . The MLS IWC sensitivity thresholds are  $0.1 \text{ mg m}^{-3}$  in the UT and  $0.02 \text{ mg m}^{-3}$  in the TL (Livesey et al., 2017) and will imply a small under-estimation of the IWC measured values.

Furthermore, we changed according the detection limits values in the Tables 2 and 3.

**5) Figure 1:** Panels a) and c) look identical – is that true or a mistake ?

Yes it was a mistake. We have changed the panel c) by the correct one.

**6) line 173** ‘In DJF, local maxima of Prec, IWC, WV, IWC fraction and RHI in the UT (Fig. 2) ...’

Comment: Prec is shown in Fig. 1, please note.

We modified the sentence l. 295 as:

In DJF, local maxima of Prec (Fig. 1), IWC, WV, IWC fraction and RHI in the UT (Fig. 2) are found over the main convective areas

**7) line 185** ‘According to the difference between the UT and the TL, WV decreases more with altitude over the MariCont region compared to all other tropical regions.’ ...

Comment: Can you further explain why WV decreases more with altitude over the MariCont?

WV (Figures 2b and 3b) decreases more with altitude because of the temperatures (Figures 2d and 3d). Like temperature, the saturation WV concentration decreases with altitude, leading to the decrease of the observed WV.

We answer to these questions in changing the text l.188. See answer #8) line 309.

Furthermore, we have changed the scales of Figures 2 and 3 a, b and d in order to have the same scale sample in the UT and the TL (the new figures are copied at the end of this report).

‘According to the difference between the UT and the TL’ – what do you mean with that ?

... ‘Consistently, TEMP is lower at 100 hPa (near the CPT) than at 146 hPa and its value is the lowest over the MariCont region.’

Comment: Isn't it vice versa: consistently with the lower TEMP over the MariCont region the WV is lower ?

We answer to these questions in changing the text l.188. See answer #8) line 309.

**8) line 188** ‘While WV decreases by more than 8 ppmv in the TL over the MariCont region compared to the UT, the RHI in the TL reaches high values (RHI ~100 %) highlighting a saturated environment ...’ Comment: This is not a surprise – the high RHI is consistent with the low TEMP. Please note.

We have changed by the following sentences starting line 309:

According to the difference between the UT and the TL, WV decreases more with altitude over the MariCont region compared to all other tropical regions. Consistently, TEMP is lower at 100 hPa (near the CPT) than at 146 hPa and its value is the lowest over the MariCont region. The IWC fraction is larger over MariCont than elsewhere in the tropics in the TL (near 78%). While WV decreases by more than 8 ppmv in the TL over the MariCont region compared to the UT, the RHI in the TL reaches high values (RHI ~100 %) highlighting a saturated environment over the central South America, Africa, MariCont and the Western Pacific Ocean.

With the decrease of temperature from the UT to the TL (Figs. 2 and 3) and the associated decrease of WV at saturation, the observed WV decreases by more than 11 ppmv over the MariCont region and by around 5 ppmv in other regions. In the TL, the IWC and the fraction of water in the ice form is larger over MariCont (beyond 1 mg m<sup>-3</sup> and near 78%, respectively) than elsewhere in the tropics. RHI in the TL reaches high values (RHI ~100 %) highlighting a saturated environment over the central South America, Africa, East of MariCont and the Western Pacific Ocean. In comparison to other tropical regions, the larger IWC over the MariCont can be explained by (i) the larger condensation of water vapour associated with the larger temperature drop from the UT to the TL, and (ii) a larger transport of ice into the TL by deep convection.

**9) line 192** ‘To investigate the vertical distribution and the diurnal cycles of water species in the TL, we have defined seven tropical convective zones shown in Figure 4’

Comment: It would be better to introduce Fig. 4 earlier (see comment on line 46).

We introduced the MariCont, earlier in Fig.1 in the introduction. However, we decided to present the choice of the study zones after having shown the global tropical characteristics observed in Figs.1, 2 and 3. Thus, this is only from Figs. 1, 2 and 3 that we decided to selected the 7 study zones presented in Fig. 7.

We have changed line 315 in order to explain more how we have chosen these study zones:

‘To investigate the vertical distribution and the diurnal cycles of water species in the TL, we have defined from results presented Fig.1–3, seven tropical convective zones shown in Figure 4:’

**10) line 211** ‘RHI is lower in the UT than at the TL by ~10 % ‘Comment: This is not a new finding – please provide references.

We have inserted a new reference Fueglistaler et al. (2009) and modified the selected sentence in line 338:

RHI is lower in the UT than at the TL by ~10 % (Fueglistaler et al., 2009) (Figs. 2d and 3d, respectively).

The reference is in the References section:

Fueglistaler, S., Dessler, A. E., Dunkerton, T. J., Folkins, I., Fu, Q. and Mote, P. W.: Tropical tropopause layer, *Rev. Geophys.*, 47(1), RG1004, doi:10.1029/2008RG000267, 2009.

**11) line 213** ‘The convective lifted ice does not sublimate as rapidly as in the UT ...’

Comment: in case of saturation or supersaturation, the ice does not sublimate at all ... as you state later in the paragraph, existing ice crystals even grow and sediment. I recommend to rephrase the sentence to provide a clear picture of the processes.

We changed the text line 338 by :

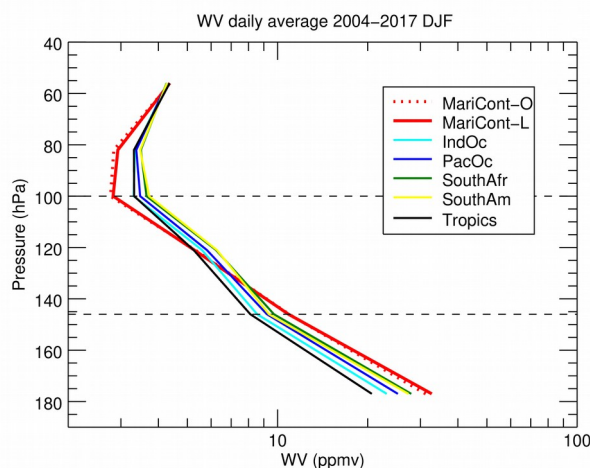
Since the UT is on average sub-saturated, convective-lifted ice can sublimate and can be seen as a source of WV. At the TL, as the atmosphere is in average close to saturation (RHI ~100%) over SouthAm, SouthAfr, MariCont and the Western Pacific Ocean (Fig. 3), the convective-lifted ice is statistically more often transported into a saturated or supersaturated region. In such context, the associated ice hydrometeors grow and sediment, and can also be transported down by convective downdrafts. These processes contribute to the loss of ice in this layer. Furthermore, the TL is the level of greatest dehydration because of supersaturation with respect to ice (Jensen et al., 1996; Jensen et al., 2005). In supersaturation conditions, the excess of water vapour can condensate on existing ice crystals (or form new ones in presence of condensation nucleus) allowing ice crystals to grow and sediment which dehydrates the layer. Conversely, hydration may occur in the LS (if reached by convection) because this layer is subsaturated with respect to ice (Khaykin et al., 2009; Allison et al., 2018; Dauhut et al., 2018).

By the way: dehydration → dehydration (line 215)

We modified the error.

**12) Figure 5** The water vapor axis in panel b), I would recommend to use a logarithmic scale to make the differences in the TL better visible.

We changed the figure 5 b by the following new one with the logarithmic scale:



**13) line 237** ‘Over land, all regions under consideration show a better efficiency to inject ice in the UT during Day than during N. is  $\beta_x$  the IWC background.’

Comment: Something is wrong with the end of the sentence (marked in blue).

We modified the typo into line 367:

Over land, all regions under consideration show a better efficiency to inject ice in the UT during Day than during Night.  $\beta_x$  is considered as the IWC background.

**14) line 259** ‘Deep convection does not inject directly WV in the UT’.

Comment: Is that true ? Look for example the recently appeared paper:

Convective hydration in the tropical tropopause layer during the StratoClim aircraft campaign: Pathway of an observed hydration patch Keun-Ok Lee et al. <https://www.atmos-chem-phys-discuss.net/acp-2018-1114/>

The effect of deep convection on the WV in the UT and TL is primarily that the convection injects mainly ice, some of which sublimates to increase WV. This has been demonstrated in studies in Cloud Resolving Models, e.g. simulations of the Hector convective system to the north of Australia (Dauhut et al., 2015). In that case, the onset of the WV increase is delayed by 1-3 hours with respect to the onset of deep convection (~12:00 LT). For this reason, the space correlation between Prec and WV is very low compare to the space correlation between Prec and IWC (see results in section 3.3 and Table 1). For that reason, we now focus on the diurnal cycle of ice (rather than of WV) and on the amount of ice injected into the UT and TL traced by Prec.

However, as we say on the introduction, with some specific condition, some WV can enter directly into the LS by overshoots. Infact, WV injection into the TTL would be totally excluded only if the TTL is always supersaturated. For that reason, we changed the sentence line 259 by the new one line 391:

Deep convection does not inject directly WV in the UT. Modelling studies from Cloud Resolving Models based on the Hector convective system in North of Australia (Dauhut et al., 2015) show that WV in the UT and TL is produced by ice sublimation. The onset of the WV increase is delayed by 1-3 hours with respect to the onset of deep convection (~12:00 LT).

To sum up, the space correlation  $R$  between  $IWC_{Day,Night}^{146}$  and  $Prec_{Day,Night}$  ( $R \sim 0.7$ ) is larger than the space correlation  $R$  between  $WV_{Day,Night}^{146}$  and  $Prec_{Day,Night}$  ( $R \sim 0.2$ ). For that reason, we now focus on the diurnal cycle of ice and on the amount of ice injected in the UT and the TL by deep convective systems traced by Prec.

Deep convection does not inject directly WV in the UT, but injects ice which then may sublimate into WV. Modelling studies with Cloud Resolving Models illustrate the sequence of mecanisms (ice uplift, mixing, sublimation) that leads convection to hydrate initially subsaturated layers (Dauhut et al., 2015, 2018, and Lee et al., 2018). In Dauhut et al. (2015), the onset of the WV increase is delayed by 1-3 hours with respect to the onset of deep convection (~12:00 LT). Such delay can explain why  $WV_{Day,Night}^{146}$  and  $Prec_{Day,Night}$  are not spatially correlated in observations ( $R \sim 0.2$ ), while the space correlation  $R$  between  $IWC_{Day,Night}^{146}$  and  $Prec_{Day,Night}$  is stronger ( $R \sim 0.7$ ). For this reason, we now focus on the diurnal cycle of ice and on the amount of ice injected in the UT and the TL by deep convective systems traced by Prec.

**15) line 327** ‘ ... (the diagram over ocean would look different since maxima appear during local night ton).is defined as the time ...

Comment: Something is wrong with the end of the sentence (marked in blue).

We have changed the typo into line 458:

(the diagram over ocean would look different since maxima appear during local night).  $t_{on}$  is defined as the time when Prec starts to...

16) **Figure 10** What is the dashed red line in panel b) ?

332 ‘ (see the period of proportionality in Fig. 10).’ Is this the dashed red line ? Please indicate.

The red dashed line represents when  $t_{on} \approx t_{on}^B$  (i. e. when the diurnal minimum of IWC occurs at the same time as the diurnal minimum of Prec). For more explanation about the red dashed line, we deleted one of the confuse back square and changed the caption of Fig.10 as follow:

**Figure 2: Methodology to estimate the diurnal cycle of ice water content (IWC) over land: (a) diurnal cycle of precipitation, with  $t_{on}$  representing the minimum of precipitation ( $Prec_{min}$ ) with its associated time ( $t_{on}$ ) and Prec during the day ( $Prec_{Day}$ ) at  $t_{Day} = 13:30$  LT. (b) Diurnal cycle of  $IWC^B(t)$  in red solid line, estimated from the diurnal cycle of Prec and from the two MLS measurements of ice ( $IWC_x^B$ ), with the timing of the onset of the ice injection at  $t_{on}^B = t_{on} + \delta t^B$ .  $IWC_{max}^B$  represents the IWC maximum ( $IWC_{max}^B$ ) and  $IWC_{min}^B$ , the  $IWC_{min}^B$  when  $\delta t^B > 0$ . Note that when  $t_{on} \approx t_{on}^B$ , the diurnal cycle of IWC is the red dashed line.**

17) **line 333** ‘This hypothesis considers deep convection represented by Prec as the main process bringing ice into the UT and the TL.’

Comment: Could you please further justify the hypothesis that deep convection is the main process bringing ice into the UT and the TL – what is with the thin cirrus that are not included in your analysis? They can also bring (or form) ice in these regions.

We modified the selected sentence (section 2). We explained that MLS is also able to measure thin cirrus. Thus, ice composing cirrus formed by deep convection during the growing phase of the convection are included in our calculation. However, our method is not able to make the difference between ice including cirrus formed by convection and cirrus formed by other processes.

Thus, we changed line 464:

This hypothesis considers deep convection represented by Prec as the main process bringing ice into the UT and the TL during the growing phase of the convection.

For more explanation we also changed the line 280:

Whereas the water budget in the TL is mostly affected by deep convection, Prec is driven by both shallow and deep convection. Deep convection can affect water vapour and ice in the UT and the TL whereas Prec measurements include the contribution of both shallow convection (that does not reach the UT) and deep convection (reaching the UT and the TL).

18) **line 332, 334** P(t) and P<sub>x</sub> : P means Prec ?

We corrected this typo. P = Prec.

19) **line Figure 11** The colors in the panels are differently defined:

(a) red – IWC<sub>p</sub>, blue – IWP, black – Prec

(b) red – IWC, blue – PIWP, black – Prec

In the caption (and text) you define pIWP, IWC, Prec. Please clarify.

We corrected it.

20) **line 356** 4.2 Validation of the method with SMILES measurements

Comment:

(a) The SMILES instrument is important for the evaluation of the method, but it is not introduced (for example in Section 2) and no references are given. Please insert a brief description of the IWC detection method and the uncertainties of the measurements to convincingly demonstrate that SMILES is suitable to evaluate the data analysis method applied here.

We created a new session, l. 267, into the Section 2) to introduce SMILES and we added some references.

### 2.3 SMILES

The Superconducting Submillimeter-Wave Limb-Emission Sounder (SMILES) was a Japanese atmospheric limb sounding instrument on board the International Space Station (ISS) platform. SMILES measurements of ice are used in this study. The instrument measured IWC between 120 and 80 hPa and the measurement of tropospheric ice, the partial Ice Water Path (pIWP) integrated between 1000 and 180 hPa, during the short period of October 2009 to April 2010. As ISS follows a low Earth orbit, with about 15 orbits a day, the ice measurements in the troposphere and tropopause layer over the entire 40°N-40°S band can be provided in about two months. Thus, the austral convective season of DJF is enough to covers the entire tropical band. Furthermore, as each orbit is drifted about 20 min earlier each day, the entire diurnal cycle of ice can be provided during this period. In the present study, SMILES measurements will be used as reference of diurnal cycle of ice and will be compared to the climatology of the diurnal cycle of ice estimated in the UT and the TL.

References about previous SMILES studies are presented later in the section 4.2, and in the references:

The diurnal cycle of IWC and pIWP calculated from SMILES has shown the well separated signal over tropical land and ocean (Millán et al., 2013; Jiang et al., 2014).

Jiang, J. H., Su, H., Zhai, C., Janice Shen, T., Wu, T., Zhang, J., et al.: Evaluating the Diurnal Cycle of Upper-Tropospheric Ice Clouds in Climate Models Using SMILES Observations. *J. Atmos. Sci.* 72, 1022–1044., doi:10.1175/JAS-D-14-0124.1, 2014.

Millán, L., Read, W., Kasai, Y., Lambert, A., Livesey, N., Mendrok, J., Sagawa, H., Sano, T., Shiotani, M. and Wu, D. L.: SMILES ice cloud products, *J. Geophys. Res. Atmospheres*, 118(12), 6468–6477, doi:10.1002/jgrd.50322, 2013.

**(b) Validation** : I suggest to better use ‘Evaluation’, since also the SMILES measurements are no absolute proof.

We changed « Validation » by « Evaluation » in the title of the session. l. 486.

**21) line 393** ‘NOAA Interpolated Outgoing Longwave Radiation (OLR) during DJF 2009-2010 is consistent with the fact that the convective activity grows higher over land than over ocean (not shown).’

Comment: What do you mean with ‘consistent’? Even if a figure is not presented, the ranges of OLR over land and over ocean should be specified.

We clarified (l. 523) the selected sentence into:

NOAA Interpolated Outgoing Longwave Radiation (OLR) during DJF 2009-2010 is lower over land (mean OLR between 195 and 215  $W m^{-2}$ ) than over ocean (between 235 and 270  $W m^{-2}$ ) which is consistent with the more intense land convective activity compared to that of oceans.

**22) line 417**

how = show

modified

23) line 423 ‘Table 4 presents ton TL,  $\Delta t$  TL, IWCmin TL and  $\Delta IWC$  TL...’

Comment: ton TL is not shown in Table 4.

We modified the wrong sentence in the caption of Table 4:

Table 4: As a function of the delay ( $\delta t = 0, 1, 2, \text{ or } 3 \text{ h}$ ) between the beginning of the Prec onset and the IWC onset in the tropical tropopause layer (TL): **time of the onset of the ice injection in the TL** ( $t_{on}^{TL}$ ), **duration of the injection of ice in the TL** ( $\Delta t^{TL}$ ), **minimum amount of ice in the TL** ( $IWC_{min}^{TL}$ ) and **amount of ice injected into the TL** ( $\Delta IWC^{TL}$ ) as a function of the 6 study zones and averaged over the land and ocean zones ( $\mu(Lands \text{ ZonesTropics})$ ,  $\mu(Oceans \text{ ZonesTropics})$ , respectively) during DJF from 2004 to 2017. The bolded values highlight the most important  $IWC_{min}^{TL}$  and  $\Delta IWC^{TL}$  and the associated regions.

24) line 440 ‘... all these results are consistent with the OLR showing strongest values over region having highest OLR signal (not shown).’ ???

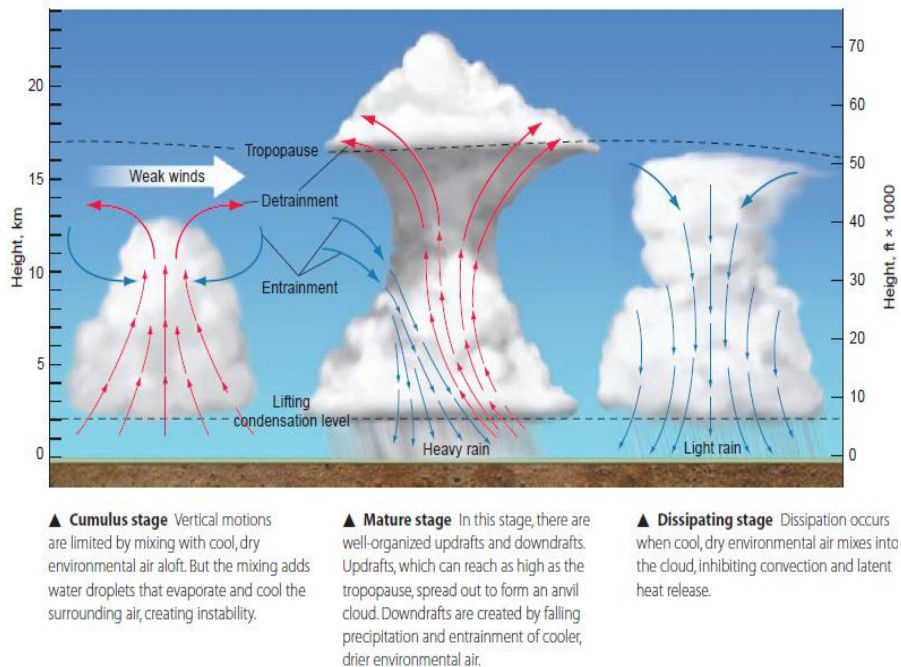
We decided to remove this confuse sentence line 572:

Furthermore, all these results are consistent with the OLR from the NOAA, showing strongest values over region having OLR signal such as over lands (not shown).

25) line 447 ‘... convective processes during the dissipating stage,...’

Comment: As long as convection is active, how can the ice clouds are in a dissipating stage ? Or do you mean ‘... decreasing convective processes ...’ ? See also line 452

‘Dissipating stage’ is a term used to describe the period during which the convection is decreasing (Takahashi and Luo, 2014). During this stage, downdraft processes are more important than updraft processes. For instance, we present Figure R1 the definition of the convective dissipating stage. (During the dissipating stage, the ascending convective transport weakens or disappears and the other processes such as sublimation, sedimentation and large-scale transport and mixing then act to decrease the local ice concentrations.)



#### 4.28 Stages in the development of an air-mass thunderstorm

The three development stages of an air-mass thunderstorm are the cumulus, mature, and dissipating stages. Each stage has characteristic vertical winds and precipitation.

Figure R1. Illustration and definition of the cumulus stage, mature stage and dissipating stage of an air-mass thunderstorm from <http://geography.name/thunderstorms-2/>.

To be more clear, we added line 122:

Finally, the influence of the  **downdraft**  convective dissipating stage on the decreasing phase of the IWC diurnal cycle in the UT and the TL is discussed in Section 5 and conclusion will be drawn in Section 6.

and line 584:

This loss can be caused by several processes including sedimentation,  **downdraft**  convective processes during the dissipating stage, sublimation into water vapour or horizontal advection and mixing.

**26) line 483** ‘Other processes may play a minor role such as the decrease of the temperature in the TTL, increasing the saturation ratio and allowing the crystal nucleation and growth, or the bring of ice in the UT and TL by horizontal advection.’

Comment: How do you know that these processes are minor? Do you know their order of magnitude in comparison to deep convection? From my feeling your conclusion is right, but for an ensured statement I think an estimate of the other processes is needed.

Firstly, we changed in the text:

Other processes may play a minor role such as the decrease of the temperature in the TTL, increasing the saturation ratio and allowing the crystal nucleation and growth, or the  **transport**  of ice in the UT and TL by horizontal advection.

Then, to answer to your questions and to be more clear in the text, we added the following sentences:

The decreasing phase of the ice diurnal cycle is also evaluated with Prec and discussed. While,  **it is difficult to quantify the impact of other processes than convective processes on the diurnal cycle of ice in the UT and the TL, we are able to assess that the deep convection impacts on the depletion of ice during the decreasing phase of the ice diurnal cycle (from Table 5: 97 % in the UT over the MariCont and ~80 % in averaged UT and TL over other regions). Thus, Prec is also considered to be a good proxy of the decreasing phase of the convection, especially over the MariCont-L region in the UT (to within 3 %, according to Table 5), and convective processes are the main processes impacting the decreasing phase of the diurnal cycle of ice. Furthermore, our study has shown that the estimated diurnal variation of ice is the largest in the regions (identified from TRMM) where the diurnal variation in temperature is also the largest although horizontal transport may play a role, but it cannot be quantified using our methodology.**

**27) line 491** ‘.. the injection of ice over the MariCont-L into the UT and the TL ... is the greatest in the tropics.’

Comment: So your finding is that deep convection is the major process feeding the ‘stratospheric fountain’ and not large- scale three-dimensional circulation, yes ? You mentioned in the abstract that the relative importance of the two processes continues to be debated – so I think you could better pronounce the importance of your finding. This is true also for line 495

Our study is mainly focus on the UT and TL layers and does not conclude on the water or ice entry into the LS. Water vapour entering the stratosphere may be determined by large-scale temperatures or perhaps by overshooting convection. However, results in our study could provide some new information to other studies about the water entrance into the LS via deep convection. For that reason, we decided to change the sentence l 623:

It has been shown that the injection of ice over the MariCont-L into the UT and the TL ( $AIWC^{UT} = 3.34 \text{ mg m}^{-3}$ ,  $AIWC^{TL} = 0.56\text{-}0.42 \text{ mg m}^{-3}$ ) is the greatest in the tropics.  **This**

injection of ice could have a strong importance on the amount of ice entering into the LS and feeding what has been called the 'stratospheric fountain' (Newell and Gould-Stewart, 1981) observed over the MarCont region.

We also changed the sentence line 629:

In summary, while the importance of deep convective processes and large-scale three-dimensional circulation processes on the ice and water injection up to the UT, TL and LS are still debated, our study shows that the ice diurnal cycle in the UT and the TL is mainly governed by vertical processes linked to the convective activity that are much stronger than other processes such as e.g. horizontal mixing, sublimation, sedimentation, ...

Two papers that might be of interest for you study:

Robrecht et al. (2018): Mechanism of ozone loss under enhanced water vapour conditions in the mid-latitude lower stratosphere in summer, ACPD.

Smith et al. (2017):

A Case Study of Convectively Sourced Water Vapor Observed in the Overworld Stratosphere over the United States, JGR.

Thank you. However we do not use these two papers in the references because, these are both about water vapour injection into the stratosphere and its consequences (in midlatitudes), while we are focusing on the UT and the TL layers only.

## RESPONSES TO THE ANONYMOUS REFEREE #2

### General remarks.

1)\* The introduction places the study into the context of stratospheric water vapour and related problematics. With that, in my opinion, the obtained results are of limited relevance for the control of stratospheric water budget. The stratospheric entry of water is mostly driven by minimum temperature at the Cold Point Tropopause and, to a much smaller extent, by injection of ice into subsaturated environment above this level. The CPT level corresponds to 82 hPa level of MLS (as can be clearly seen in Fig. 5a), whereas the analysis is performed for 146 and 100 hPa levels. The ice water detrained below CPT may have very little or no impact on stratospheric water: even if the injected ice crystals sublimate before settling down, the amount of water vapour ascending into the stratosphere would be limited by the colder temperatures at CPT level. Moreover, large-scale convection may lead to additional cooling of CPT at diurnal and intra-diurnal time scales thereby further limiting the cross-tropopause transport of water. I believe the above considerations should be discussed in the context of the role of deep convection of stratospheric water. It would also be useful to compare the results regarding IWC obtained for 100 hPa with those for 82 hPa level.

We modified the whole introduction in order to move the focus away from stratospheric water vapour (Referee #2) (and to provide more justification for the work that is presented (Referee #1)).

2)\* On the base of comparison between TRMM Prec and TRMM OPF diurnal cycles, Prec is shown to be a good proxy of deep convection during its growing phase. Could you clarify why the OPF data as such could not be used for the IWC analysis?

Indeed, OPF would be a better proxy of deep convection reaching the TL than Prec. However, the OPF fields were only available for the period studied in Liu and Zipser (2005),

namely from January 1998 to November 2000 and from December 2001 to December 2003, and were not accessible to the scientific community. Consequently, we ought to find another proxy covering the 2004-2017 period. However, it could be very interesting to find other instruments available during 2004-2017, able to build the same estimation than the OPFs (originally calculated from the combination of TRMM observations and different instruments detailed in Liu and Zipser (2005)).

In our study, Prec has been measured by TRMM over the same period than IWC from MLS: 2004-2017. In addition to the comparison of Prec and IWC, we also show that Prec behaves as OPF during the growing phase of the deep convection in austral convective seasons of DJF.

We have inserted a new paragraph l. 438:

In summary, although OPFs are representative of deep convection reaching the TL, OPFs developed and presented in Liu and Zipser (2005) are not available during our study period of 2004-2017. However, our results in this section have shown that during the growing stage of deep convection, Prec is a good proxy of convection reaching the TL over land and ocean. Thus, as Prec is available in time coincidence with MLS IWC and WV over 2004-2017, we will use Prec to interpret the time evolution of IWC in the UT and the TL.

### Specific remarks.

**3) l. 18-19.** The purpose of the method is missing in this sentence, i.e. “We propose a method for..using...”

We modified the specified sentence line 20 into:

We propose a method that uses Prec as a proxy of deep convection bringing ice up to the UT and TL during the growing stage of the convection, in order to estimate the amount of ice injected in the UT and the TL, respectively.

**4) l. 165.** The title of Sect. 3.1 should be more specific.

We changed it line 284 into:

Tropical distribution of Prec and water budget in the UT and TL

**5) l. 180.** The statement regarding a ubiquitous subsaturation in the Austral convective regions is surprising. Consider that the RH product of MLS may have a substantial dry bias at 82 hPa since it is based on MLS temperature profiles. The latter, in turn, do not resolve the sharp temperature minimum at CPT, which leads to underestimation of RHI at this level. While the geographical distribution of MLS RH could be fairly accurate, the quantitative statements based on these data should be avoided. A correct way to infer RHI values from MLS measurements would be to compute them from WV profiles of MLS and temperature profiles from a reanalysis data set with sufficient vertical resolution in the TTL, e.g. MERRA-2.

MLS provides RHI measurements with a vertical resolution of about 5 km, which . The validation of the RHI product from MLS is presented in Read et al. (2007). More precisely, from 316–0.002 hPa, RHI is derived from the standard products of water and temperature using the Go-Gratch ice humidity saturation formula. Furthermore, our analysis is climatological, thus RHI is a climatological value. It may be possible that  $RHI > 100\%$  on some specific locations and periods.

Our results presented in Fig. 2 show that RHI is below 100% in the UT (146 hPa) whereas RHI is reaching 100% in the TL (100 hPa). Thus, we modified the sentence l. 297 into:

The RHI is higher over land than over ocean but RHI never exceeds 100% at 146 hPa, on average at  $2^\circ \times 2^\circ$  resolution (consistently with the RHI tropical vertical profil shown by Fueglistaler et al., 2009). The MariCont region exhibits the highest RHI with values close to 100%.

6) 1.203. Since Fig. 5a shows the profiles at the native MLS pressure levels, a correct inference on the CPT pressure would be 83 hPa  $\pm$  half width of MLS weighting function.

With the information given by MLS on temperature observations, we are not able to give the pressure level of the CPT to better than the half-width at the maximum of the associated averaging kernel. In Fig. 5a, we expect the CPT to be between 100 and 82 hPa that is already widely known. In order to support these statements, we decided to add 2 references: Fueglistaler et al. (2009) (their Figure 5 shows temperatures at different pressure levels) and Kim and Son (2012) (their Figure 3 shows CPT temperatures).

We modified in section 3.2, line 335, the following sentence:

In Fig. 5a, the tropical CPT is found in the pressure range of 82 hPa  $\pm$  half width of the associated averaging kernel. Figure 6 presents the tropical tropopause pressure defined by NCEP and shows an averaged pressure ( $\sim$  100-115 hPa) close to the pressure given by MLS at 100 hPa, named the TL in this study. Based on previous studies (Fueglistaler et al., 2009 and Kim and Son, 2012) and fig 6, we can nonetheless narrow the TTL range to 100-80 hPa.

We added Kim and Son (2012) into the References section line 701:

Kim, J. and Son, S.-W. Tropical Cold-Point Tropopause: Climatology, Seasonal Cycle, and Intraseasonal Variability Derived from COSMIC GPS Radio Occultation Measurements. *J. Climate*, 25, 5343–5360, doi: 10.1175/JCLI-D-11-00554.1, 2012.

Furthermore, Fig. 5a indicates which region has the lowest/highest temperature profiles. In order to complete this Figure, we choose to present Fig. 6 which gives the pressure level of the tropopause.

7) 1.204-207 and Fig. 6. What is the relevance of this information in the context of Sect.3.2 entitled “Water budget in the UT and TL”? Please clarify.

In Fig. 6, we found the tropopause between 100 and 115 hPa what is close to the layer that we called “TL”, defined at 100 hPa. Fig. 6 shows the longitudinal pressure differences of the Tropopause and completes Fig. 5. From Fig. 6, the Tropopause is found to be **the lowest** over the MariCont whereas, from Fig. 5a, the tropopause is found to be **the coldest** over the MariCont.

Furthermore, from Fig. 6, the tropopause is found to be higher over ocean than over land.

Thus, these two figures provide complementary information on the tropical tropopause layer area. From Fig. 5a, the CPT is near 82 hPa for all study zones, whereas the tropopause defined by NCEP is close to 100 hPa.

We have inserted a new paragraph in this section, l. 327:

To investigate the processes in the UT and TL which drive the water budget, the vertical profiles of TEMP, WV, IWC and RHI are shown for the different study zones in Figure 5. To complete the comparison between the study zones, the DJF average of the tropopause pressure level is represented over all the tropics in Figure 6 from the National Centers For Environmental Prediction (NCEP).

In Fig. 5a, the tropical CPT is found between 100 and 80 hPa consistently with previous results presented in e.g. Fueglistaler et al. (2009) and Kim and Son (2012). The tropical tropopause defined by NCEP (Fig. 6) is close to the level given by MLS at 100 hPa we named the TL in this study ( $\sim$  100-115 hPa). Furthermore, the tropopause pressure shown in Fig.6 is lower (higher altitude) over ocean than over land. While the pressure at the tropopause over West Pacific, South Arabia, Caribbean sea present is the lowest ( $\sim$ 105

hPa). Furthermore, the tropopause is the coldest (Fig. 5a) and has the highest pressure (lower altitude) (Fig. 6) over the MariCont.

**8) 1.282-283.** The section title refers to UT level, whereas the first line reads “...convection reaching the tropopause ...”

We modified the specified sentence line 143 into:

1. 298 :

In this section, we quantify the link between deep convection reaching the UT and Prec.

**9) Sect. 4.2.** For consistency, the description of SMILES instrument should be introduced in Sect. 2. Please clarify how the full diurnal coverage is ensured with ISS platform.

This point has been detailed in the response to the referee #1 (point 20)

**10) Figure 1.** Color scales of 1a and 1b should be the same. Figure 1c is a duplicate of 1a. Technical corrections.

This point has been detailed in the response to the referee #1 (point 5).

**11) 1.175.** Maximal => maximum

Done.

**12) 1.213.** Convectively-lifted?

Done

**13) 1.221.** Spatial correlation

Done

**14) 1.223.** Consider rephrasing the sentence ending with “... WV and IWC in the UT and Prec is analyzed”.

1.238, we modified the specified sentence line 351 into:

~~In order to quantify the relationship between deep convection and the budget of water injected in the UT, the correlation between both WV and IWC in the UT and Prec is analysed.~~

This section presents the relationship between deep convection and the water vapour and ice injected in the UT.

**15) 1.237-238.** Broken sentence

See point #13 of the Referee #1.

**16) 1.376.** try “before reaching”

Done.

**17) 1.417** sentence unclear

1.433, we changed :

~~Thus, the ice background is similar over land and ocean in the UT but there is 4 times more ice injected in the UT over land than over ocean.~~

The new sentence is line 549 :

Thus, the ice minima are of similar amplitudes over land and ocean in the UT but the amount of ice injected in the UT is about 4 times greater over land than over ocean..

18) 1.879. 30 N => 30S

Done.

19) 1.882. sentence unclear

l.1040, we changed :

All the data have been filtered with a 6-h running average.

The new sentence is line 1041:

Data have been smoothed out using 6-h running average.

# Ice injected up to the Tropopause by Deep Convection: 1) in the Austral Convective Tropics

Iris-Amata DION<sup>1</sup>, Philippe RICAUD<sup>1</sup>, Peter HAYNES<sup>2</sup>, Fabien CARMINATI<sup>3</sup> and Thibaut DAUHUT<sup>4</sup>

<sup>1</sup> CRNM, Météo-France - CNRS, Toulouse, 31057, France

5 <sup>2</sup> DAMTP, University of Cambridge, Cambridge, CB3 0WA, United Kingdom

<sup>3</sup> Met Office, Exeter Devon EX1 3PB, United Kingdom

<sup>4</sup> Laboratoire d'Aérodynamique, Université de Toulouse, CNRS, UPS, Toulouse, 31400, France

Correspondence to: Iris-Amata DION (iris.dion@meteo.fr)

**Abstract.** The impact of deep convection on the water budget from the tropical Upper Troposphere (UT, around 146 hPa) to the Tropopause Level (TL, around 100 hPa) is investigated. The contribution of deep convection to the amount of water vapor and ice in the Tropical Tropopause Layer (TTL) from the tropical upper troposphere (UT, around 146hPa) to the Tropopause Level (TL, around 100hPa) is investigated. Ice water content (IWC) and water vapour (WV) measured in the UT and the TL by the Microwave Limb Sounder (MLS, Version 4.2) are compared to the precipitation (Prec) measured by the Tropical Rainfall Measurement Mission (TRMM, Version 007). The two datasets, gridded within  $2^\circ \times 2^\circ$  horizontal bins, have been analyzed during the austral convective season: December, January and February (DJF) from 2004 to 2017. MLS observations are performed at 01:30 and 13:30 Local Solar Time whilst the Prec dataset is constructed with a time resolution of 1 hour. The new contribution of this study is to provide a much more detailed picture of the diurnal variation of ice than is provided by the very limited (2 per day) MLS observations. Firstly, we show that IWC represents 70 and 50% of the total water in the tropical UT and TL, respectively and that Prec is spatially highly correlated with IWC in the UT (Pearson linear coefficient  $R=0.7$ ). We propose a method that uses Prec as a proxy of deep convection bringing ice up to the UT and TL during the growing stage of the convection, in order to estimate the amount of ice injected in the UT and the TL, respectively. We validate the method using ice measurements from the Superconducting Submillimeter-Wave Limb-Emission Sounder (SMILES) during the period DJF 2009-2010. Next, the diurnal amount of IWC injected into the UT and the TL by deep convection is calculated by the difference between the maximum and the minimum in the estimated diurnal cycle of IWC in these layers and over selected convective zones. Six tropical highly convective zones have been chosen: South America, South Africa, Pacific Ocean, Indian Ocean, and the Maritime Continent region, split into land (MariCont-L) and ocean (MariCont-O). IWC injection is found to be 2.73 and 0.41  $\text{mg m}^{-3}$  over tropical land in the UT and TL, respectively, and 0.60 and 0.13  $\text{mg m}^{-3}$  over tropical ocean in the UT and TL, respectively. The MariCont-L region has the greatest ice injection in both UT and TL (3.34 and 0.42-0.56  $\text{mg m}^{-3}$ , respectively). The MariCont-O region has less ice injection than MariCont-L (0.91  $\text{mg m}^{-3}$  in the UT and 0.16-0.34  $\text{mg m}^{-3}$  in TL), but has the highest diurnal minimum value of IWC in the TL (0.34-0.37  $\text{mg m}^{-3}$ ) among all oceanic zones.

## 1 Introduction

Water vapour (WV) is one of the main greenhouse gases and has an important impact on the climate. WV in the stratosphere has a direct radiative impact on surface temperatures and it participates in the warming of the troposphere and the cooling of the stratosphere (Solomon et al., 2010; Birner and Charlesworth, 2017). It also has a strong impact on stratospheric chemistry, especially on the ozone equilibrium (Stenke and Grewe et al., 2005) as it contributes to the ozone destruction in the polar regions via the formation of polar stratospheric clouds (Fahey et al., 1989; Solomon, 1999; Vogel et al., 2011). According to observations, stratospheric WV concentrations increased by ~30% between 1980 and 2000 (Scherer et al., 2008; Hurst et al., 2011) and would increase by up to a factor of 2 over the twenty-first century (Gettelman et al., 2010; Maycock et al., 2013; Hegglin et al., 2014). After 2000, some studies have related the stratospheric WV drop in the tropics with the decrease of the Cold Point tropopause (CPT) temperature (Randel et al., 2006). It is known that tropospheric air masses and water enter the stratosphere mostly in the tropics (Fueglistaler et al., 2009). In the tropics, the minimum of temperature at the tropopause regulates the stratospheric WV. The tropical tropopause layer (TTL) is defined by the layer between the level of maximum convective outflow (10-12 km, ~200 hPa) that closely corresponds to a minimum in ozone and the CPT temperature (16-17 km, ~100 hPa) (Gettelman and Forster, 2002; Mehta et al., 2008; Birner and Charlesworth, 2017). Among this layer, in the present study, we separate and define the Tropopause Level (TL, ~17 km, ~100 hPa) to the Upper Troposphere level (UT, ~14 km, ~146 hPa). In the tropics, the exchange between the troposphere and the stratosphere is larger over the region called Maritime Continent (MariCont), the region between the Indian Ocean and the West Pacific (Newell and Gould-Stewart, 1981), than elsewhere on earth. Newell and Gould-Stewart (1981) have called this strong exchange over the MariCont region, the 'stratospheric fountain'. In the tropics, transport from troposphere to stratosphere (TST) occurs through a combination of large-scale three-dimensional circulation and deep convection (e.g. Fueglistaler et al., 2009; Randel and Jensen, 2013). The relative importance of the two processes continues to be debated (e.g. Alcala and Dessler, 2002; Liu and Zipsper, 2005; Carminati et al., 2014).

Water is one of the rare chemical compounds to be present in 3 phases (solid, liquid and gas) in the atmosphere. However, in the TTL, because of the very low temperature, water is only found as vapor and ice.

In the tropics, the Brewer Dobson Circulation (BDC) leads the variations of WV at the tropopause (Potter and Holton, 1995) to propagate upward in the tropical stratosphere, a phenomenon called the "Tape Recorder effect" (Mote et al., 1996). The globally average TTL and stratospheric WV is controlled by the TTL very low temperatures which regulate the lowest saturation mixing ratio that the air masses encounter (Hartmann et al., 2001; Fueglistaler et al., 2009; Khaykin et al., 2013) and impacts the water phase change. The amount of water injected into the UT-LS is still not well quantified. Sherwood and Dessler (2000) present a hypothesis on the stratospheric hydration and dehydration as two different processes which occur on different time scales and involving vertical and horizontal air mixing into the TL. Ueyama et al. (2015) have shown that tropical waves dehydrate the TL (at 100 hPa level) by 0.5 ppmv while the cloud microphysical processes and convection moisten the TL by 0.7 and 0.3 ppmv, respectively. Some authors have shown that fast overshoots from deep convection

65 transports very rapidly water upward (from few minutes to one hour) into the stratosphere (Pommereau et al., 2010; Dauhut et al., 2015). Liu and Zipser (2005) have found that 1.3% of tropical convection systems reach 14 km and 0.1% of them may even penetrate the 380 K potential temperature level which corresponds to the CPT. Dauhut et al. (2015) have estimated that 18% of the water mass flux across the 380 K potential temperature level is due to overshooting deep convection. Avery et al. (2017) have also suggested that tropical convective ice cloud and associated cirrus sublimating at unusually high altitudes  
70 might also have a role in stratospheric hydration. The other path for water is the slow vertical advection ( $300 \text{ m.month}^{-1}$ ) governed by radiative heating (Holton and Gettelman, 2001; Gettelman and Forster, 2002; Corti et al., 2006; Fueglistaler et al., 2009). Once into the UT or the TL, the amount of the relative humidity of the layer impacts the ice nucleation, growth and sedimentation (Peter et al., 2006). The amount of water in solid phase brought by deep convection into the UT-LS is not well quantified and the associated processes are not well understood. Thus, the aim of the present study is to quantify the role  
75 of the deep convection on the hydration and dehydration of the TL. For that, in this study, we focus on the diurnal injection of ice in the UT and the TL from the deep convective activity.

The diurnal cycle is one of the most fundamental modes of variability of the global climate system and is associated with large and well-defined variations in the solar forcing (Yang and Slingo, 2001). The amplitude of the surface thermal diurnal cycles in the tropics is ten times stronger than the amplitude of the surface thermal annual cycle (Beucher, 2010) and the  
80 diurnal cycle of deep convection is mainly governed by the surface thermal diurnal cycle. Understanding the diurnal cycle of the total water in the tropical UT, TL and LS contributes to characterize the total water exchange between the UT and the LS in the tropics. Many studies (e.g. Jiang et al., 2014) have shown that the diurnal cycle of ice in the UT is linked to the diurnal cycle of the convection. The maximum of deep convection in the UT has been shown to peak in the local afternoon over land and in the local early morning over ocean (Liu and Zipser, 2005). Based on these studies and with data from the space-borne  
85 Microwave Limb Sounder (MLS) instrument, Carminati et al. (2014) studied the diurnal cycle of WV and ice in the TL over Africa and South America and have shown the presence of a strong diurnal signal over the two continents. Sunceth et al. (2017) have shown the differences in the diurnal cycles of CPT altitudes and CPT temperatures over tropical land and ocean. The diurnal cycle of temperature has also been studied in the TL (Khaykin et al., 2013) showing that the amplitude of temperature anomalies increases with the intensity of the convection.

90 In summary, the processes driving the total water diurnal cycle are different in the UT and at the TL, e.g. only the deepest convection directly impacts water content at the TL and saturation is more frequent at the TL than in the UT. Since the total water diurnal cycle in the TTL is still not well described in global models (Jiang et al., 2014), space-borne observations may improve our understanding of the processes occurring in this layer.

The present study addresses the question relative to the diurnal cycle of total water over tropical deep convective areas.  
95 Africa and South America are two land regions of intense deep convective activity in the tropics, together with the MariCont region (made of lands and oceans). However, the deep convective systems occur more frequently and strongly over the MariCont region (Liu and Zipser, 2015) than over the other continental zones. It is known that excess of energy received by tropical surfaces is mainly balanced and transferred over land by convection toward mid-latitudes and over ocean by both

100 convection and oceanic circulation. However, over the MariCont region, seas and oceans currents transferring energy toward  
mid-latitudes are slowed down and blocked by the thousands of islands. Consequently, the excess of energy in the oceanic  
surface over the MariCont region is mainly balanced by transfer from convection. The diurnal cycle of WV and ice has  
already been studied over Africa and South America and over the whole tropical band (see e.g. Liu and Zipser, 2009; Millán  
et al., 2013; Carminati et al., 2014). The MariCont region is the driest and coldest area at the CPT and the water budget in the  
TL over the MariCont region separating MariCont land and MariCont ocean is still unknown. Furthermore the physical  
105 mechanism governing the diurnal cycle of convection and surface precipitation over ocean is still an open question.  
In order to understand the total water diurnal cycle in the TL, we first use 13 years of the ice water content (IWC) and WV  
measurements from MLS (Version 4.2x) and surface precipitations (Prec) from the TRMM instrument. Then, we use WV,  
IWC, total water ( $\Sigma W = WV + IWC$ ), relative humidity with respect to ice (RHI) and temperature (TEMP) from MLS and  
Prec from TRMM over the period 2004 to 2017 in order to better understand the water fraction ( $IWC/\Sigma W$ ) in the UT (~146  
110 hPa) and the TL (~100 hPa, around the CPT). The relationships between surface precipitation and the processes in the UT  
and the TL are investigated. Our study intends to evaluate the mechanisms affecting the diurnal cycle of total water in the TL  
above land and ocean with a particular emphasis over the MariCont region due to its topographical complexity. Thus, the  
diurnal cycle of ice (provided by MLS but with very poor time resolution) is improved and better understood thanks to the  
relation with the diurnal cycle of precipitation (provided by TRMM with a much better time resolution).  
115 The main datasets used are presented in Section 2. The methodology developed to establish the link between the diurnal  
cycle of surface processes and the diurnal cycle of water in the UT and TL is presented in Section 3. The estimated diurnal  
injection of IWC in the UT and TL from deep convective activity is presented in Section 4. Finally, the influence of the  
convective dissipating stage on the decreasing phase of the IWC diurnal cycle in the UT and the TL is discussed in Section 5  
and conclusion will be drawn in Section 6. This paper contains many abbreviations and acronyms. To facilitate reading, we  
120 compile them in the Appendix.

Water vapour (WV) is one of the main greenhouse gases and has an important impact on the climate, particularly in the  
tropics. WV concentrations are limited by temperature which regulate the saturation mixing ratio in air masses (Hartmann et  
al., 2001; Fueglistaler et al., 2009; Khaykin et al., 2013). In consequence, WV is much smaller in the upper troposphere (UT)  
125 and stratosphere than in the lower troposphere. However, despite the small concentrations, the WV distribution in the  
tropical upper troposphere (e.g. Soden et al., 2008) and stratosphere (e.g. Solomon et al., 2010) plays an important role on  
climate, including the determination of the overall radiative balance of the troposphere. The WV distribution in this region of  
the atmosphere is strongly coupled to the distribution of cirrus clouds which despite being thin, can have a significant effect  
on the overall thermal balance of the troposphere (e.g. Zhou et al., 2014). The tropical upper stratosphere and lower  
130 stratosphere recognized as a distinct region of the atmosphere – the Tropical Tropopause Layer (TTL) – is defined by the  
layer between the level of maximum convective outflow (10-12 km, ~200 hPa) that closely corresponds to a minimum in  
ozone and the cold point temperature (CPT) (16-17 km, ~100 hPa) (Gettelman and Forster, 2002; Mehta et al., 2008; Birner

and Charlesworth, 2017). Within the TTL, a complex set of physical processes interact to determine the distribution of temperature, WV and clouds, and other radiatively active chemical species (e.g. Fueglistaler et al., 2009; Randel and Jensen, 2013). The TTL is important in determining several aspects of troposphere-to-stratosphere exchange and therefore determining the chemical composition of the stratosphere. Much attention has therefore been focused on the role of TTL processes in setting the value of WV concentrations that enter the stratosphere. In particular, there has been an ongoing debate of the relative importance of large-scale processes in which air masses move slowly from troposphere to stratosphere within the large-scale three-dimensional circulation and dehydrates as it encounters very cold temperatures and small-scale processes, in which convection injects WV (and ice) directly into the TTL and, the stratosphere, with potentially hydrating impact. The relative importance of the three-dimensional circulation processes and convective processes continues to be debated (e.g. Alcala and Dessler, 2002; Liu and Zipser, 2005; Carminati et al., 2014).

For instance, Ueyama et al. (2015) have shown that tropical waves dehydrate the TTL by 0.5 ppmv while the cloud microphysical processes and convection moisten the TTL by 0.7 and 0.3 ppmv, respectively. Some authors have shown that fast overshoots from deep convection transport very rapidly water upward (from few minutes to one hour) into the stratosphere (Pommereau et al., 2010; Dauhut et al., 2015). Liu and Zipser (2005) have found that 1.3% of tropical convection systems reach 14 km and 0.1% of them may even penetrate the 380 K potential temperature level which corresponds to the CPT. Avery et al. (2017) have also suggested that tropical convective ice cloud and associated cirrus sublimating at unusually high altitudes might also have a role in stratospheric hydration. The other path for water entering the lower stratosphere (LS) is the slow vertical advection ( $300 \text{ m.month}^{-1}$ ) governed by radiative heating (Holton and Gettelman, 2001; Gettelman and Forster, 2002; Corti et al., 2006; Fueglistaler et al., 2009). Once into the UT or the TTL, the amount of the relative humidity of the layer impacts the ice nucleation, growth and sedimentation (Peter et al., 2006).

Whilst there is observational evidence for convective hydration events (Liu and Zipser, 2005; Pommereau et al., 2010; Avery et al., 2017) and convective hydration of the stratosphere has been clearly corroborated by state-of-the-art numerical simulations (e.g. Dauhut et al., 2015), the quantitative role of convective hydration in determining water vapour concentrations in the main body of the stratosphere remains uncertain. One approach has been to combine observational estimates of overshooting convection frequency with information from short-localised duration numerical simulations. Using this approach, Dauhut et al. (2015) have estimated that 18% of the water mass flux across the 380 K potential temperature level is due to overshooting deep convection. Another has been to include estimates of convective penetration, e.g. from satellite observations into large-scale trajectory calculations. The conclusions are sensitive to the assumptions made but, for example, Wright et al. (2013) and Schoeberl et al. (2018), both conclude that the effect of convective penetration on WV concentrations in the stratosphere is very weak, essentially because most air masses that are moistened by convective injection are subsequently dehydrated during encounter cold temperatures on the large-scale before they reach the main body of the stratosphere.

Whether or not convective processes play a direct role in determining stratospheric WV concentrations, it is clear that, moving from the lower TTL to the upper TTL, convective-scale processes play an increasingly important role in determining

the distributions of WV and of cirrus. Representing convective-scale processes in global models used for weather climate prediction is challenging, and it is important where possible to evaluate model representations by finding observed characteristics of WV and cirrus in the TTL that can be usefully compared to model simulations. One opportunity is provided by diurnal variations. The time scale is of course very different to the decadal and longer timescales of interest in climate prediction, but the short time scale has the advantage of providing time series with many cycles which is therefore well characterised statistically. The diurnal cycle is one of the most fundamental modes of variability of the global climate system and is associated with large and well-defined variations in the solar forcing (Yang and Slingo, 2001). The amplitude of the surface thermal diurnal cycles in the tropics is ten times stronger than the amplitude of the surface thermal annual cycle (Beucher, 2010) and the diurnal cycle of deep convection is mainly governed by the surface thermal diurnal cycle. Understanding the diurnal cycle of the total water in the tropical UT, TTL and LS contributes to characterize the total water exchange between the UT and the LS in the tropics. Many studies (e.g. Jiang et al., 2014) have shown that the diurnal cycle of ice in the UT is linked to the diurnal cycle of the convection. The maximum of deep convection in the UT has been shown to peak in the local afternoon over land and in the local early morning over ocean (Liu and Zipser, 2005). Based on these studies and with data from the space-borne Microwave Limb Sounder (MLS) instrument, Carminati et al. (2014) studied the diurnal cycle of WV and ice in the TTL over Africa and South America and have shown the presence of a strong diurnal signal over the two continents. Suneeth et al. (2017) have shown the differences in the diurnal cycles of CPT altitudes and CPT temperatures over tropical land and ocean. The diurnal cycle of temperature has also been studied in the TTL (Khaykin et al., 2013) showing that the amplitude of temperature anomalies increases with the intensity of the convection.

In summary, the processes driving the total water diurnal cycle are different in the UT and at the tropopause layer, e.g. only the deepest convection directly impacts water content at the tropopause layer and saturation is more frequent at the tropopause layer than in the UT. Since the total water diurnal cycle in the tropopause layer is still not well described in global models (Jiang et al., 2014), space-borne observations may improve our understanding of the processes occurring in this layer. This provides motivation for the study presented in this paper, in which we consider the diurnal cycle of ice in the TTL, for which limited, but nonetheless valuable data is provided by the MLS instrument.

The aim of the present study is to quantify the role of the deep convection on the hydration and dehydration of the TTL. For that, we focus on the diurnal injection of ice in the tropical UT and the tropopause layer from the deep convective activity and address the question relative to the diurnal cycle of total water over tropical deep convective areas.

Africa and South America are two land regions of intense deep convective activity in the tropics, together with the Maritime Continent region (MariCont, the region made of lands and oceans, between the Indian Ocean and the West Pacific, presented by the red box in Fig. 1). However, the deep convective systems occur more frequently and strongly over the MariCont region (Liu and Zipser, 2015) than over the other continental zones. It is known that excess of energy received by tropical surfaces is mainly balanced and transferred over land by convection toward mid-latitudes and over ocean by both convection and oceanic circulation. However, over the MariCont region, seas and oceans currents transferring energy toward mid-latitudes are slowed down and blocked by the thousands of islands. Consequently, the excess of energy in the oceanic surface

over the MariCont region is mainly balanced by transfer from convection. The diurnal cycle of WV and ice has already been studied over Africa and South America and over the whole tropical band (see e.g. Liu and Zipser, 2009; Millán et al., 2013; Carminati et al., 2014). The MariCont region is the driest and coldest area at the CPT and the water budget in the TTL over the MariCont region separating MariCont land and MariCont ocean is still unknown. Furthermore the physical mechanism governing the diurnal cycle of convection and surface precipitation over ocean is still an open question.

In order to understand the total water diurnal cycle up to the TTL, we first use 13 years of the ice water content (IWC) and WV measurements from MLS (Version 4.2x) and surface precipitations (Prec) from the TRMM instrument. Then, we use WV, IWC, total water ( $\sum W = WV + IWC$ ), relative humidity with respect to ice (RHI) and temperature (TEMP) from MLS and Prec from TRMM over the period 2004 to 2017 in order to better understand the water fraction ( $IWC/\sum W$ ) in the UT (~146 hPa) and the tropopause layer (TL, ~100 hPa, around the CPT). The relationships between surface precipitation and the processes in the UT and the TL are investigated. Our study intends to evaluate the mechanisms affecting the diurnal cycle of total water in the TL above land and ocean with a particular emphasis over the MariCont region due to its topographical complexity. Thus, the diurnal cycle of ice (provided by MLS but with very poor time resolution) is improved and better understood thanks to the relation with the diurnal cycle of precipitation (provided by TRMM with a much better time resolution).

The main instruments used are presented in Section 2. The methodology developed to establish the link between the diurnal cycle of surface processes and the diurnal cycle of water in the UT and TL is presented in Section 3. The estimated diurnal injection of IWC in the UT and TL from deep convective activity is presented in Section 4. Finally, the influence of the convective dissipating stage on the decreasing phase of the IWC diurnal cycle in the UT and the TL is discussed in Section 5 and conclusion will be drawn in Section 6. This paper contains many abbreviations and acronyms. To facilitate reading, we compile them in the Appendix.

## 2 Datasets Instruments

### 2.1 MLS

MLS is a microwave instrument aboard the NASA's Earth Observing System (EOS) Aura platform (Livesey et al., 2017), measuring in a limb viewing geometry to maximize signal intensities and vertical resolution. The MLS instrument is aboard a sun-synchronous near-polar orbiter completing 233 revolution cycles every 16 days giving a daily global coverage with about 14 orbits. Aura is crossing the equator at 01:30 local time (LT) and 13:30 LT. Among all the atmospheric parameters measured by MLS, we focus on: IWC, WV, TEMP and RHI. IWC ( $\text{mg m}^{-3}$ ) is valid between 215 and 82 hPa. Although IWC ( $\text{mg m}^{-3}$ ) is valid between 215 and 82 hPa, the number of scientifically-exploitable measurements at 82 hPa within a  $2^\circ \times 2^\circ$  pixel is not significant. In our study, we will only use two levels to analyze IWC, at 180 and 100 hPa. WV (ppmv) is valid between 316 and 0.002 hPa, TEMP (K) between 261 and 0.001 hPa and RHI (%) between 1000-1.0 hPa. The MLS IWC

sensitivity thresholds do not allow to detect low ice content such as cirrus outflow associated with convective events. Consequently, MLS IWC sensitivity will mostly be able to detect ice from convective cores. Following Livesey et al. (2017), we will not consider IWC measurements less than  $0.02 \text{ mg m}^{-3}$ . The MLS IWC sensitivity thresholds are  $0.1 \text{ mg m}^{-3}$  in the UT and  $0.02 \text{ mg m}^{-3}$  in the TL (Livesey et al., 2017) and will imply a small under-estimation of the IWC measured values.

The MLS v4.2x data processing validated by Livesey et al. (2017) presents significant and minor differences with the previous MLS version. The total random noise in v4.2x IWC is larger than the one in v2.2. Compared with the v3.3 of MLS (used for instance in Carminati et al., 2014), the v4.2 improves IWC composition profiles in cloudy regions especially in the upper troposphere over the tropics and improves the WV at global scale (Livesey et al., 2017).

Level 2 data quality tests (filter and data screening) from the v4.2x have been applied to WV, IWC, RHI, and TEMP as suggested by Livesey et al. (2017). The MLS measurements estimated from the averaging kernels (Livesey et al., 2017) are used to characterize the distribution of the four parameters on two layers: one at 146 hPa (UT) and one at 100 hPa (TL). The vertical resolution of the IWC measurements is  $\sim 3 \text{ km}$ , the horizontal resolution is  $\sim 300 \text{ km}$  and  $7 \text{ km}$  along and across the track, respectively. The WV vertical resolution is  $2.5 \pm 1.2 \text{ km}$  and the WV along track horizontal resolution is between  $170$  and  $350 \text{ km}$ . The TEMP vertical resolution is  $4.5 \text{ km}$ .

In the study of Carminati et al. (2014), a  $10^\circ \times 10^\circ$  resolution was chosen with seven years of MLS data processed with version 3.3 (v.3.3). In our study, MLS data have been averaged over a much longer period (2004 to 2017) in a much higher horizontal resolution of  $2^\circ \times 2^\circ$  ( $\sim 200 \times 200 \text{ km}$ ). In each  $2^\circ \times 2^\circ$  bin, and for the 13 years average, any bin with less than 60 measurements in the daytime (Day at 13:30 LT) or the nighttime (Night at 01:30 LT) datasets is excluded in order to have significant statistics. Thus, the maximum of measurements per bin during the 13 years period is  $\sim 470$  and the minimum is fixed to be 60. The number of measurements over the MariCont region is on average the lowest over the tropics. Consistent with Carminati et al. (2014) and Liu and Zipser (2005), we use the difference between the MLS measurements performed during the Day and the Night to study the “Day minus Night” (Day–Night) signal.

## 2.2 TRMM

The TRMM satellite was launched in November 1997 ([https://trmm.gsfc.nasa.gov/publications\\_dir/publications.html](https://trmm.gsfc.nasa.gov/publications_dir/publications.html)). TRMM carried 5 instruments: a 3-sensor rainfall suite, the precipitation radar, the TRMM Microwave Imager, the Visible and Infrared Scanner and 2 related instruments, the Lightning Imaging Sensor and the Clouds and the Earth’s Radiant Energy System. In our study, we use the Algorithm 3B42 producing the TRMM merged high quality to infrared precipitation and root-mean-square precipitation-error estimation with the TRMM version 007. The rainfall level 3 measurements ( $\text{mm hr}^{-1}$ ) are vertically integrated precipitation (Prec). TRMM Prec data are provided in the tropics within a  $0.25^\circ \times 0.25^\circ$  horizontal resolution extending from  $50^\circ\text{S}$  to  $50^\circ\text{N}$ . TRMM datasets used in our study in coincidence with the MLS period of measurements from 2004 to 2017. In order to compare to the MLS measurement, we degraded the TRMM resolution to  $2^\circ \times 2^\circ$  in averaging the TRMM measurements in each box of  $2^\circ \times 2^\circ$  of MLS. Furthermore, as TRMM follows an orbit

precession, shifting few minutes per day, the 24-hour diurnal cycle can be averaged over the period of study, with 1-hour resolution over the 24 hour diurnal cycle.

## 2.3 SMILES

270 The Superconducting Submillimeter-Wave Limb-Emission Sounder (SMILES) was a Japanese atmospheric limb sounding instrument on board the International Space Station (ISS) platform. SMILES measurements of ice are used in this study. The instrument measured IWC between 120 and 80 hPa and the measurement of tropospheric ice, the partial Ice Water Path (pIWP) integrated between 1000 and 180 hPa, during the short period of October 2009 to April 2010. As ISS follows a low Earth orbit, with about 15 orbits a day, the ice measurements in the troposphere and tropopause layer over the entire 40°N-  
275 40°S band can be provided in about two months. Thus, the austral convective season of DJF is enough to covers the entire tropical band. Furthermore, as each orbit is drifted about 20 min earlier each day, the entire diurnal cycle of ice can be provided during this period. In the present study, SMILES measurements will be used as reference of diurnal cycle of ice and will be compared to the climatology of the diurnal cycle of ice estimated in the UT and the TL.

## 3 Relationship between Prec and water budget in the austral convective UT and TL

280 In this section, we analyze the relationships between Prec and the water budget in the UT and the TL during the DJF season, highly convective season of the southern hemisphere. Whereas the water budget in the TL is mostly affected by deep convection, Prec is driven by both shallow and deep convection. Deep convection can affect water vapour and ice in the UT and the TL whereas Prec measurements include the contribution of both shallow convection (that does not reach the UT) and deep convection (reaching the UT and the TL).

### 285 3.1 Tropical distribution of Prec and water budget in the UT and TL

The daily averaged  $((D+N)/2)$  Prec measured by TRMM at the resolution of  $0.25^\circ \times 0.25^\circ$  and  $2^\circ \times 2^\circ$  (the same horizontal resolution as MLS) are shown in Figures 1a and b, respectively. The fine structure of the horizontal distribution of Prec at the high resolution ( $0.25^\circ \times 0.25^\circ$ ) over South Africa, South America, Western Pacific Ocean and the Maritime Continent are degraded when considering Prec at low resolution ( $2^\circ \times 2^\circ$ ). Figure 1c presents the Local Solar Time (evaluated for each bin of  $0.25^\circ \times 0.25^\circ$ ) at which the diurnal cycle of Prec reaches its maximum in TRMM observations showing the large variability and complexity of the diurnal maximum of Prec over the tropics. The daily averages of IWC, WV, IWC fraction ( $IWC/\Sigma W$ ), TEMP and RHI from MLS in the tropics are shown in Figure 2 for the UT (at 146 hPa) and Figure 3 for the TL (100 hPa).

In DJF, local maxima of Prec (Fig. 1), IWC, WV, IWC fraction and RHI in the UT (Fig. 2) are found over the main convective areas: South America, South Africa, MariCont, North of Australia, along the Inter-Tropical Convergence Zone (ITCZ) and the South Pacific Convergence Zone (SPCZ). Maximum values of Prec, IWC, WV and RHI over the whole tropics are located over the MariCont (and North Australia) (Figs. 1a and b and Figs. 2a, b, c and e). Minima of Prec, IWC, WV, IWC fraction and RHI are found over Eastern Pacific Ocean and South Atlantic Ocean. Over MariCont region, we

observe the maximum of tropical IWC and the minimum of temperature (Figs. 2a and d). The IWC fraction shows that, over the region of high Prec ( $> 0.20 \text{ mm h}^{-1}$ ), up to 70% of the  $\Sigma W$  is composed of ice. ~~The RHI is higher over land than over ocean but does not reach saturation (RHI  $< 100\%$  at  $2^\circ$  resolution).~~ The RHI is higher over land than over ocean but RHI never exceeds 100% at 146 hPa, on average at  $2^\circ \times 2^\circ$  resolution (consistently with the RHI tropical vertical profil shown by Fueglistaler et al., 2009). The MariCont region exhibits the highest RHI with values close to 100%. In summary, there is a strong spatial link between Prec and water (IWC and WV) in the UT.

In the TL (Fig. 3), IWC is lower than in the UT ( $\sim 3 \text{ mg m}^{-3}$  at 146 hPa vs  $< 1 \text{ mg m}^{-3}$  at 100 hPa) but the horizontal distribution of IWC is correlated with the horizontal distribution of Prec and shows maxima over South America, South Africa, the MariCont region and Western Pacific Ocean. The main difference between the UT and the TL is the minimum of WV observed over the MariCont region ( $> 8 \text{ ppmv}$  at 146 hPa and  $< 3 \text{ ppmv}$  at 100 hPa). ~~According to the difference between the UT and the TL, WV decreases more with altitude over the MariCont region compared to all other tropical regions. Consistently, TEMP is lower at 100 hPa (near the CPT) than at 146 hPa and its value is the lowest over the MariCont region. The IWC fraction is larger over MariCont than elsewhere in the tropics in the TL (near 78%). While WV decreases by more than 8 ppmv in the TL over the MariCont region compared to the UT, the RHI in the TL reaches high values (RHI  $\sim 100\%$ ) highlighting a saturated environment over the central South America, Africa, MariCont and the Western Pacific Ocean. With the decrease of temperature from the UT to the TL (Figs. 2 and 3) and the associated decrease of WV at saturation, the observed WV decreases by more than 11 ppmv over the MariCont region and by around 5 ppmv in other regions. In the TL, the IWC and the fraction of water in the ice form is larger over MariCont (beyond  $1 \text{ mg m}^{-3}$  and near 78%, respectively) than elsewhere in the tropics. RHI in the TL reaches high values (RHI  $\sim 100\%$ ) highlighting a saturated environment over the central South America, Africa, East of MariCont and the Western Pacific Ocean. In comparison to other tropical regions, the larger IWC over the MariCont can be explained by (i) the larger condensation of water vapour associated with the larger temperature drop from the UT to the TL, and (ii) a larger transport of ice into the TL by deep convection.~~

To investigate the vertical distribution and the diurnal cycles of water species in the TL, we have defined, from results presented Fig.1–3, seven tropical convective zones shown in Figure 4: South America (SouthAm,  $0^\circ\text{N}-30^\circ\text{S}$ ), South Africa (SouthAfr,  $0^\circ\text{N}-30^\circ\text{S}$ ), Pacific Ocean (PacOc,  $0^\circ\text{N}-30^\circ\text{S}$ ;  $180^\circ\text{W}-150^\circ\text{W}$ ), Indian Ocean (IndOc,  $0^\circ\text{N}-30^\circ\text{S}$ ;  $60^\circ\text{E}-90^\circ\text{E}$ ), MariCont ( $10^\circ\text{N}-15^\circ\text{S}$ ;  $90^\circ\text{E}-160^\circ\text{E}$ ), MariCont land (MariCont-L) and MariCont ocean (MariCont-O). Land and ocean over the study zones have been separated using the Solar Radiation Data (SoDa, <http://www.soda-pro.com/web-services/altitude/srtm-in-a-tile>), providing a TIFF image with values from the Shuttle Radar Topography Mission (SRTM) Digital Elevation Model. Each zone is defined at a horizontal resolution of  $2^\circ \times 2^\circ$ .

### 3.2 Water budget in the UT and the TL

330

To investigate the processes in the UT and TL which drive the water budget, the vertical profiles of TEMP, WV, IWC and

RHI are shown for the different study zones in Figure 5. To complete the comparison between the study zones, the DJF average of the tropopause pressure level is represented over all the tropics in Figure 6 from the National Centers For Environmental Prediction (NCEP).

335 In Fig. 5a, the tropical CPT is found between 100 and 80 hPa consistently with previous results presented in e.g. Fueglistaler et al. (2009) and Kim and Son (2012). The tropical tropopause defined by NCEP (Fig. 6) is close to the level given by MLS at 100 hPa we named the TL in this study (~ 100-115 hPa). Furthermore, the tropopause pressure shown in Fig.6 is lower (higher altitude) over ocean than over land. While the pressure at the tropopause over West Pacific, South Arabia, Caribbean sea present is the lowest (~105 hPa). Furthermore, the tropopause is the coldest (Fig. 5a) and has the highest pressure (lower altitude) (Fig. 6) over the MariCont. Regarding WV, the tropical UT is more humid than the TL: the decrease from the UT at 146 hPa to the TL at 100 hPa is about 7 ppmv for WV, and 1 mg m<sup>-3</sup> for IWC (the two dashed lines in Figs. 5b and c, respectively). These results are consistent with previous studies all presented in Fueglistaler et al. (2009). RHI is lower in the UT than at the TL by ~10 % (Fueglistaler et al., 2009) (Figs. 2d and 3d, respectively). Since the UT is on average sub-saturated, convective-lifted ice can sublimate and can be seen as a source of WV. At the TL, as the atmosphere is in average close to saturation (RHI ~100%) over SouthAm, SouthAfr, MariCont and the Western Pacific Ocean (Fig. 3), the convective-lifted ice is statistically more often transported into a saturated or supersaturated region. In such context, the associated ice hydrometeors grow and sediment, and can also be transported down by convective downdrafts. These processes contribute to the loss of ice in this layer. Furthermore, the TL is the level of greatest dehydration because of supersaturation with respect to ice (Jensen et al., 1996; Jensen et al., 2005). In supersaturation conditions, the excess of water vapour can condensate on existing ice crystals (or form new ones in presence of condensation nucleus) allowing ice crystals to grow and sediment which dehydrates the layer. Conversely, hydration may occur in the LS (if reached by convection) because this layer is subsaturated with respect to ice (Khaykin et al., 2009; Allison et al., 2018; Dauhut et al, 2018).

340

345

350

### 355 3.3 Spatial correlation between Prec and water in the UT

In order to quantify the relationship between deep convection and the budget of water injected in the UT, the correlation between both WV and IWC in the UT and Prec is analysed. This section presents the relationship between deep convection and the water vapour and ice injected in the UT. We have calculated the Pearson linear correlation coefficient  $R$  between the horizontal distribution of Prec and both IWC and WV at 146 hPa during the Day, the Night and the Day-Night over the study zones (see Table 1). We denote Prec, IWC and WV at 146 hPa during Day, Night and Day-Night, by  $Prec_x$ ,  $IWC_x^{146}$  and  $WV_x^{146}$ , respectively (where  $x$ = Day, Night or Day-Night). The spatial correlation between IWC and Prec is defined by the following equation:

$$IWC_x^{146} = \alpha_x \times Prec_x + \beta_x \quad (1)$$

where  $\alpha_x$  is the regression coefficient and  $\beta_x$  is the offset.

365 The spatial correlation for the 6 zones is shown in Table 1. The spatial correlation of  $IWC_{Day}^{146}$  and  $IWC_{Night}^{146}$  with Prec is high ( $R \sim 0.7-0.9$ ) over SouthAm, SouthAfr, PacOc and IndOc and smaller ( $R \sim 0.5 - 0.6$ ) over the MariCont region (MariCont-L, MariCont-O and MariCont). The spatial inhomogeneity of the MariCont surface with thousands of islands, seas and coastal areas may probably explain the lower space correlation between the Prec and  $IWC^{146}$ . The regression coefficient between  $Prec_x$  and  $IWC_x$  (Table 1)  $\alpha_x$ , can be interpreted as the efficiency of the convective system to inject ice in the UT.

370 Comparing  $\alpha_x$  in Day and Night conditions, SouthAfr, SouthAm, MariCont-L, MariCont-O and MariCont stand out with larger Day values ( $\alpha_D = 7.5-15.0 \text{ mg m}^{-3} \text{ mm}^{-1} \text{ h}$ ) than IndOc and PacOc or than Night values ( $\alpha_N = 4.7-7.7 \text{ mg m}^{-3} \text{ mm}^{-1} \text{ h}$ ). Over land, all regions under consideration show a better efficiency to inject ice in the UT during Day than during Night.  $\beta_x$  is considered as the IWC background. Over land and ocean regions,  $\beta_x$  is close to zero.  $\beta_{Day}$  is the highest over the MariCont-L ( $1.1 \text{ mg m}^{-3}$ ) and null over SouthAm ( $0.0 \text{ mg m}^{-3}$ ). Over the oceans, there is no significant differences between  $\beta_{Day}$  and  $\beta_{Night}$  for the injected ice in the UT, except over PacOc.

375 Following Liu and Zipser (2009) and Carminati et al. (2014), we also study the difference between Day and Night, to obtain information on the  $IWC^{146}$  diurnal cycle. Figure 7 shows the  $Prec_{Day-Night}$ ,  $IWC_{Day-Night}^{146}$  and  $WV_{Day-Night}^{146}$ , respectively. Convective regions such as SouthAm, SouthAfr, even along the ITCZ, are characterized by a positive Day–Night signal in  $Prec_{Day-Night}$  and  $IWC_x^{146}$  with values greater than  $0.10 \text{ mm hr}^{-1}$  and  $0.20 \text{ mg m}^{-3}$ , respectively (Figs. 7a and b). The spatial correlation  $R$  between  $Prec_{Day-Night}$  and  $IWC_{Day-Night}^{146}$  is greater over the 3 land zones ( $R \geq 0.6-0.7$ ) than over the 3 ocean zones ( $R \leq 0.1-0.5$ ). MariCont-O region shows the highest oceanic correlation ( $R \sim 0.5$ ) compared to the PacOc and IndOc regions ( $R = 0.2$  and  $0.1$ , respectively). The low  $R$  values over IndOc and PacOc could be explained by: i) the low  $IWC_{Day-Night}$  variability compared to the high  $Prec_{Day-Night}$  variability observed over ocean and ii) the low amplitude of the deep convection diurnal cycle over ocean (Liu and Zipser, 2005). We could hypothesize that  $IWC^{146}$  over the MariCont-O is more influenced by local deep convection than over IndOc and PacOc. However, considering  $IWC^{146}$  and Prec during Day and Night independently, we find good correlation over the ocean ( $\sim 0.6-0.8 \text{ mg m}^{-3}$ ).

385 The spatial correlation  $R$  between  $Prec_x$  and  $WV_x^{146}$  remains low in all configurations, with values of  $0.-0.5$  (Table 1). The spatial correlation between the  $WV_{Day-Night}^{146}$  and  $Prec_{Day-Night}$  shows an average over the 7 study zones of  $\mu_{Zones} \sim 0.07$  with small negative correlations over SouthAm and SouthAfr and with a regression coefficient  $\alpha_x$  between  $WV^{146}$  and Prec calculated to be  $\alpha_x = 0$  (Table 1). We conclude that WV is not spatially correlated with the diurnal cycle of the deep convection. These results are consistent with results from Liu and Zipser (2009) and Carminati et al. (2014) showing that the Day–Night signal of WV measured by MLS is very different with the Day–Night signal of IWC measured by MLS in the UT over land.

390 Deep convection does not inject directly WV in the UT, but injects ice which then may sublime into WV. Modelling studies with Cloud Resolving Models illustrate the sequence of mechanisms (ice uplift, mixing, sublimation) that leads convection to

395

hydrate initially subsaturated layers (Dauhut et al., 2015, 2018, and Lee et al., 2018). In Dauhut et al. (2015), the onset of the WV increase is delayed by 1-3 hours with respect to the onset of deep convection (~12:00 LT). Such delay can explain why  $WV_{Day, Night}^{146}$  and  $Prec_{Day, Night}$  are not spatially correlated in observations ( $R \sim 0.2$ ), while the space correlation  $R$  between  $IWC_{Day, Night}^{146}$  and  $Prec_{Day, Night}$  is stronger ( $R \sim 0.7$ ). For this reason, we now focus on the diurnal cycle of ice and on the amount of ice injected in the UT and the TL by deep convective systems traced by Prec.

### 3.4 Diurnal cycle of Prec

This section is presenting the diurnal cycle of Prec over the 6 study zones during the Southern Hemisphere convective season (DJF) from 2004 to 2017 over land and ocean, respectively (Figures 8a and b).

405 Over land, the amplitude (peak to peak) of the Prec diurnal cycle varies between 0.2 and 0.3 mm h<sup>-1</sup>, with simultaneous minima between 08:00 and 09:00 LT within the regions. MariCont-L area shows the driest minimum (0.09 mm h<sup>-1</sup>) and the wettest and latest maximum (16:00-17:00 LT, 0.385 mm h<sup>-1</sup>). SouthAm and SouthAfr maxima are found at 14:00-15:00 LT and 15:00-16:00 LT, respectively.

410 Over ocean, the amplitude of the Prec diurnal cycle varies between 0.08 and 0.1 mm h<sup>-1</sup>, with simultaneous minima between 17:00 and 18:00 LT. However, the maxima are spread between 01:00 and 06:00 LT.

The main difference between Prec diurnal cycle over tropical ocean and land are: i) morning maximum over ocean compared to early afternoon over land, ii) peak to peak diurnal cycle of Prec is larger over land than over ocean and iii) minima can be twice lower over land (0.1 mm h<sup>-1</sup>) than over ocean. The comparison of the Prec diurnal cycle over MariCont and MariCont-O or MariCont-L highlights the importance of analyzing separately the diurnal cycle over land and over ocean in this region, 415 because MariCont-O and MariCont-L have two distinct behaviours which are hidden when the diurnal cycle is only considered over the MariCont global area.

### 3.5 Time correlation between Prec and IWC during the growing convective phase in the UT

In this section, we quantify the link between deep convection reaching the UT and Prec. The diurnal cycle of Prec is 420 compared to the diurnal cycle of the frequency of overshooting precipitation features (OPFs) events (i.e. the proportion of all OPF events that occurs in various ranges of time of day, adapted from Figure 3 of Liu and Zipser (2005) from global satellite radar measurements) over land (Figure 9a) and ocean (Figure 9b) in the tropical band (20°S-20°N). The OPFs considered by Liu and Zipser (2005) are tropical deep convective systems penetrating the tropical TL (called  $Z_{tropopause}$  in Liu and Zipser (2005)). The OPFs are calculated from measurements from January 1998 to November 2000 and from December 2001 to 425 December 2003 based on TRMM precipitation radar (PR) measured reflectivity into precipitation features (PFs) and using the method described by Nesbitt et al. (2000). The OPFs can be identified thanks to the high vertical resolution of the TRMM PR.

Over land, the diurnal cycle of Prec and OPF shows a maximum at 16:00-17:00 LT and a minimum at 09:00-10:00 LT (Fig. 9a). The duration of the growing phase, defined as the period between the minimum and the maximum of Prec, is the same for OPF and Prec, and lasts  $\Delta t = 7$  hours. The major difference in the diurnal cycles of Prec and OPF occurs after the growing phase: the fraction of OPF decreases more rapidly than that of Prec and stops decreasing around 00:00 LT whereas that of Prec continues to decrease. This difference can be explained by the contribution to Prec of 1) the convection that does not reach the stratosphere and 2) the mature phase of the OPF that produces stratiform rain for some hours after the overshooting time. These results over land are consistent with Pereira et al. (2005) showing that the shallow convection is associated with 10% of precipitation over Amazonian region. Although OPF and Prec diurnal cycles are not calculated over the same study period, we can deduce from the present analysis that during the growing phase, the time evolution of Prec is a good proxy for the time evolution of deep convection reaching the TL (OPFs).

Over ocean, the sea surface temperature (SST) does not have a strong diurnal cycle (less than  $\sim 1$  K) with a peak in the early afternoon (e.g., Chen and Houze, 1997; Stuart-Menteth et al., 2003). The convective clouds usually develop after the SST peak, during the afternoon and during the night with a maximum in the early local morning. The diurnal cycle of Prec and OPF (Fig. 9b) over the ocean have a maximum over night (05:00-06:00 LT) and a minimum in the end of the afternoon (18:00-19:00 LT for the OPF and 20:00-21:00 LT for the Prec). The diurnal cycles of OPF and Prec over the ocean show similar amplitudes in deviation from the mean. This result is consistent with Peirera et al. (2005) showing that the shallow convection is associated with only 3% of precipitation over Eastern Pacific region.

In summary, although OPFs are representative of deep convection reaching the TL, OPFs developed and presented in Liu and Zipser (2005) are not available during our study period of 2004-2017. However, our results in this section have shown that during the growing stage of deep convection, Prec is a good proxy of convection reaching the TL over land and ocean. Thus, as Prec is available in time coincidence with MLS IWC and WV over 2004-2017, we will use Prec to interpret the time evolution of IWC in the UT and the TL.

#### 4. Amount of ice injected in the UT and the TL by deep convection

In this section, we present the method we have developed to estimate the diurnal cycle of IWC in the UT ( $IWC^{UT}(t)$ ) and in the TL ( $IWC^{TL}(t)$ ) based on the diurnal cycle of Prec and on the two per day IWC measurements by MLS. Like in the previous section for OPF, we separate the diurnal cycle of IWC into a growing phase (period when deep convection develops to reach the UT and the TL), and a decreasing phase (period when deep convection dissipates). During the growing phase, Prec is a good indicator (proxy) of deep convection both over land and ocean (section 3.5). This is not true during the decreasing phase, when shallow convection can have a significant impact on Prec. Since IWC is spatially highly correlated with Prec and since the deep convection (OPFs) bringing ice into the TL increases with Prec during the growing phase, we expect ice to be injected up to the UT and the TL with a delay ( $\delta t^{UT,TL}$ ) after the onset of the deep convection  $t_{on}$  during the growing phase.

The method developed focuses on the growing stage of deep convection. We quantify the amount of ice injected to the UT

and the TL and determine the onset time of the ice injection and its duration. The amount of ice injected will be calculated from the estimation of the amplitude of the diurnal cycle of IWC in the UT and the TL.

#### 4.1 IWC diurnal cycle in the UT and TL

The method to estimate  $IWC^B(t)$  ( $B = UT$  or  $TL$ ) is presented in this section. Figure 10 illustrates the methodology to find the  $IWC^B(t)$  over land (the diagram over ocean would look different since maxima appear during local night).  $t_{on}$  is defined as the time when Prec starts to increase and  $t_{on}^B$  is defined as the time when  $IWC^B$  starts to increase. Our two main hypotheses are to assume that: i)  $IWC^B$  starts to increase later than Prec (a delay  $\delta t^B$  is assumed) because convective systems precipitate before reaching UT and TL, as follow:

$$t_{on}^B = t_{on} + \delta t^B \quad (2)$$

and ii) the  $IWC^B(t)$  is proportional to the  $Prec(t)$  during the convective growing phase (see the period of proportionality in Fig. 10). This hypothesis considers deep convection represented by Prec as the main process bringing ice into the UT and the TL during the growing phase of the convection. Based on these two hypotheses and knowing  $Prec_x$  and  $IWC_x^B$  at  $t_x$  and

$$t_{on}^B, \text{ we estimate } IWC^B(t_{on}^B) \text{ as follows: } IWC^B(t_{on}^B) = \frac{Prec(t_{on}^B)}{Prec_x} \times IWC_x^B \quad (3)$$

where  $x = Day$  or  $N$ . We use  $t_x = t_{Day}$  for land since only the Day measurement occurs during the growing phase over land, and  $t_x = t_{Night}$  over sea since only the Night measurement occurs during the growing phase over ocean. Knowing  $IWC^B(t_{on}^B)$  and  $t_{on}^B$ , the time evolution  $IWC^B(t)$  during the growing phase is then:

$$IWC^B(t) = \begin{cases} \frac{Prec(t)}{Prec(t_{on}^B)} \times IWC^B(t_{on}^B) & \text{if } Prec(t) > Prec(t_{on}^B) \\ IWC^B(t_{on}^B) & \text{else.} \end{cases} \quad (4)$$

Our method can then estimate the magnitude of the diurnal variation in the UT and the TL ( $\Delta IWC^B$ ) over different regions of the tropics:

$$\Delta IWC^B = IWC^B(t_{end}) - IWC^B(t_{on}^B) = IWC_{max}^B - IWC_{min}^B \quad (6)$$

with  $t_{end}$  being the time of the diurnal maximum of Prec.  $t_{end}$  can be considered as the time of the end for ice injection or the time from which the downdraft processes are more important than the updraft processes. Thus, we define  $\delta t_{end}^{UT}$  as the delay between  $t_{end}$  and  $t_{end}^{UT}$ . Following the hypothesis ii that considers that deep convection is the main process bringing ice into the UT and the TL, calculated  $\Delta IWC^B$  represents the amount of ice injected by deep convection in these two layers. Thus,

the duration of the injection of ice during the growing phase,  $\Delta t^B$  is then:

$$\Delta t^B = t_{end} - t_{on}^B \quad (7)$$

490 In order to validate this method, we compare the estimation of the amount of ice injected ( $\Delta IWC^B$ ) into the UT and the TL with the amount of ice measured in the troposphere and in the TL by the SMILES instrument on board the ISS during the short convective period of December 2009 to February 2010.

#### 4.2 Validation-Evaluation of the method with SMILES measurements

500 The SMILES instrument measured IWC between 120 and 80 hPa and the overall measurement of tropospheric ice, the partial Ice Water Path (pIWP) integrated between 1000 and 180 hPa, from October 2009 to April 2010. This period is an El Niño Southern Oscillation (ENSO) period, increasing the convective activity over South Africa and the Western Pacific Ocean and decreasing the convective activity over the MariCont region and South America. The diurnal cycle of IWC and pIWP calculated from SMILES has shown the well separated signal over tropical land and ocean (Millán et al., 2013; Jiang et al., 2014). The anomalies of the diurnal cycle of IWC measured by SMILES near the TL, the diurnal cycle of pIWP in the troposphere and the diurnal cycle of Prec measured during the convective period of December 2009 to February 2010 are presented in Figure 11a over the three land study zones and in Figure 11b over the three ocean study zones, both with a running average of 6 h.  $t_{on}$ ,  $t_{on}^{UT}$  and  $t_{on}^{TL}$  are the times of the minimum of Prec ( $Prec_{min}$ ), pIWP ( $pIWP_{min}$ ), and IWC ( $IWC_{min}$ ), respectively.

505 Over land, during the growing phase, pIWP is proportional to Prec (Fig. 11a). Assuming that  $IWC^{146}$  evolves like pIWC, this implies that  $t_{on}^{UT} \approx t_{on}$  ( $\delta t_{on}^{UT} = 0$ ) at  $\sim 08:00-09:00$  LT, and  $t_{end}^{UT} \approx t_{end} + \delta t_{end}^{UT}$  at  $\sim 16:00-17:00$  LT, with  $\delta t_{on}^{UT} \leq 1$  h and  $\delta t_{end}^{UT} \leq 1$  h. Then, pIWP decreasing phase follows the same time evolution as Prec reaching minima ( $Prec_{min}$  and  $pIWP_{min}$ ) around 07:00-09:00 LT. Thus, ice in the troposphere follows the same diurnal cycle as the Prec within a time resolution of one hour.

In the TL, IWC is still proportional to Prec but IWC starts to increase later than ( $\delta t_{on}^{TL} \sim 1$  h) the pIWP in the UT (Fig. 11a). After  $t_{end}$ , IWC decreases more rapidly than Prec and varies between +2 and -7 % compared to the mean between 23:00 and 510 09:00 LT. Thus, as soon as the deep convection reaches one of these two levels, ice is brought by the updraft during the growing and mature stage of the convective activity. Then, ice decreases with the downdraft of the convective dissipating stage. However, the very deep convective activity reaching the TL starts later than the deep convection reaching the UT ( $\delta t \approx 1$  h) and decreases quickly before reaching a background IWC minimum between 23:00 LT and 09:00 LT.

Over ocean during the growing phase (Fig. 11b), pIWP also increases proportionally to Prec. Assuming that  $IWC^{146}$  evolves 515 like pIWC, this implies that  $t_{on}^{UT} \approx t_{on} + \delta t_{on}^{UT}$  ( $\delta t_{on}^{UT} \geq 1$  h) at  $\sim 21:00-22:00$  LT, and  $t_{end}^{UT} \approx t_{end} + \delta t_{end}^{UT}$  at  $\sim 04:00-05:00$  LT with  $\delta t_{end}^{UT} > 1$  h. Thus, as  $\delta t_{on}^{UT} \approx \delta t_{end}^{UT}$ , the diurnal cycle of pIWP over ocean is synchronized with the diurnal cycle of Prec but delayed. In the TL and during the growing phase, IWC starts to increase later than pIWP (where  $\delta t_{on}^{TL} \approx 15$  h, Fig. 11b). This

520 result is consistent with the diurnal cycle of OPF presented in Figure 9, where OPF starts to increase with a delay  $\delta t_{on}^{TL} \approx 9$  h with respect to the increase of Prec. According to Liu and Zipser (2005), only less than 5% of OPF reach the TL, so other processes in addition to deep convection govern the ice diurnal cycle in the TL over ocean impacting on the delay between the onset of ice injection  $t_{on}^{TL}$  and the onset of the convection  $t_{on}$ . After  $t_{on}^{TL}$ , IWC takes around 13 h to reach a maximum at  $t_{end}^{TL} \sim 19:00-20:00$  LT.

525 Table 2 presents the magnitude of diurnal variation of ice, that is to say, the amount of ice injected into the UT and the TL estimated using the model presented in section 4.2 from the MLS and TRMM measurements ( $\Delta IWC^B$ ) and the magnitude of diurnal variation of ice measured by SMILES ( $\Delta pIWP$  and  $\Delta IWC_{SMILES}$ ) over the six study zones and during DJF 2009-2010.  $\Delta IWC^{UT}$  and  $\Delta IWC^{TL}$  are close to  $\Delta pIWP_{SMILES}$  and  $\Delta IWC_{SMILES}$ , respectively (with differences between 0.02 to 0.28  $\text{mg m}^{-3}$ ). Thus, during the ENSO period of DJF 2009-2010, the amount of ice injected in the UT ( $\Delta IWC^{UT}$ ) is about 2.06-2.34  $\text{mg m}^{-3}$  over land and 1.20-1.22  $\text{mg m}^{-3}$  over ocean and in the TL ( $\Delta IWC^{TL}$ ) is about 0.26-0.31  $\text{mg m}^{-3}$  over land and 0.13-0.22  $\text{mg m}^{-3}$  over ocean. NOAA Interpolated Outgoing Longwave Radiation (OLR) during DJF 2009-2010 is lower over land (mean  
530 OLR between 195 and 215  $\text{W m}^{-2}$  (not shown)) than over ocean (between 235 and 270  $\text{W m}^{-2}$ ) which is consistent with the more intense land convective activity compared to that of oceans.

In summary, our method based on the correlation between Prec from TRMM and IWC from MLS during the growing stage of the convection (presented in section 4.1) allows to estimate the amount of ice injected into the UT and the TL ( $\Delta IWC^B$ ) and has been validated with the SMILES measurements over land and ocean. These results confirm that the diurnal cycle of  
535 Prec can be used as proxy of deep convection reaching the UT and the TL during the growing stage of the deep convection. The analyses of SMILES data also suggest a good correlation of  $IWC^{UT}$  and Prec during the dissipating stage of the convection in the UT over land.

### 4.3 Amount of ice injected in the austral convective UT

Using the method presented in the previous section, 13 years of MLS and TRMM observations are analysed. Table 3  
540 presents the time of the beginning of the IWC injection in the UT ( $t_{on}^{UT}$ ), the duration of the IWC injection ( $\Delta t^{UT} = t_{end}^{UT} - t_{on}^{UT}$ ), the minimum value of IWC before the beginning of the IWC injection ( $IWC_{min}^{UT}$ ) and the amount of ice injected in the UT (equivalent to the amplitude of the IWC diurnal cycle,  $\Delta IWC^{UT} = IWC_{max}^{UT} - IWC_{min}^{UT}$ ).

Over land,  $t_{on}^{UT}$  is found during the morning at 08:00-09:00 LT whatever the land zone. However,  $\Delta t^{UT}$  is longer over MariCont-L than SouthAm and SouthAfr ( $\Delta t^{UT} = 8, 7$  and  $7$  h, respectively). Furthermore,  $IWC_{min}^{UT}$  is lower over the  
545 MariCont-L than over SouthAm and SouthAfr ( $IWC_{min}^{UT} = 1.04, 1.65$  and  $1.33$   $\text{mg m}^{-3}$ , respectively), but  $\Delta IWC^{UT}$  is greater over the MariCont-L than over SouthAm and SouthAfr ( $\Delta IWC^{UT} = 3.34, 1.99$  and  $2.86$   $\text{mg m}^{-3}$ , respectively).

Over ocean,  $t_{on}^{UT}$  is found during the evening at 17:00-18:00 LT.  $\Delta t^{UT}$  is much longer over MariCont-O than over IndOc and PacOc ( $\Delta t^{UT} = 11, 9, 9$  h, respectively). However  $IWC_{min}^{UT}$  is greater over MariCont-O than over IndOc and PacOc ( $IWC_{min}^{UT} =$

1.62, 1.01 and 1.46 mg m<sup>-3</sup> respectively) and  $\Delta IWC^{UT}$  over MariCont-O is also greater than  $\Delta IWC^{UT}$  over PacOc and IO  
550 ( $\Delta IWC^{UT} = 0.91, 0.46$  and  $0.43$  mg m<sup>-3</sup>, respectively).

Thus, the convective growing stage is quicker over land (7 h) than over ocean (10 h). These results are consistent with previous study from Takahashi and Luo (2014) showing that the time life of the mature stage of the deep convection is between 6 and 12 h after the onset of the deep convection considering North and South hemispheres over the tropics. Furthermore, while the estimated means of  $IWC_{min}^{UT}$  over land and ocean are very close (1.34 and 1.36 mg m<sup>-3</sup>, respectively),  
555 the means of the land and ocean  $\Delta IWC^{UT}$  show great differences (2.73 and 0.60 mg m<sup>-3</sup>, respectively). Thus, the ice background is similar over land and ocean in the UT but there is 4 times more ice injected in the UT over land than over ocean. Thus, the ice minima are of similar amplitudes over land and ocean in the UT but the amount of ice injected in the UT is about 4 times greater over land than over ocean. These results also show that the MariCont region is a region with greater amount of ice injection in the UT compared to other tropical deep convective areas.

#### 560 4.4 Amount of ice injected in the austral convective TL

From the method presented previously and the results from the SMILES instruments (Fig. 11), Table 4 presents  $t_{on}^{TL}$ ,  $\Delta t^{TL}$ ,  $IWC_{min}^{TL}$  and  $\Delta IWC^{TL}$  with respect to time for ice to be injected into the TL after the onset of deep convection,  $\delta t^{TL}$  over the different study zones. We propose to use  $\delta t^{TL} = 0$  to 3 h in order to keep  $\delta t^{TL}$  always shorter than  $t_{on}-t_x$ , where  $x$  is selected during the growing phase ( $x=D$  over land and  $x=N$  over ocean) in order to perform a sensitivity study of our results.

565 Over land, for all  $t_{on}^{TL}$ , the period of injection ( $\Delta t^{TL}$ ) is longer over MariCont-L than over SouthAm and SouthAfr ( $\Delta t^{TL} = 8, 7$  and  $7$  h, respectively). Depending on the  $\delta t^{TL}$  (between 0 and 3 h),  $\Delta t^{TL}$  can be between 7-8 and 4-5 h.  $\Delta IWC^{TL}$  is greater over MariCont-L than over SouthAm and SouthAfr for all the  $\delta t^{TL}$  ( $\Delta IWC^{TL} \sim 0.56-0.42, 0.26-0.13$  and  $0.40-0.24$  mg m<sup>-3</sup>, respectively). As observed in the short time period study with SMILES, the injection of ice over MariCont-L is the most intense over tropics. Furthermore, the smaller  $\delta t^{TL}$ , the longer  $\Delta t^{TL}$ , the greater  $\Delta IWC^{TL}$ .

570 Over ocean, as observed with the SMILES measurements,  $t_{on}^{TL}$  cannot be estimated with our method. However, our method is able to estimate  $\Delta t^{TL}$ ,  $IWC_{min}^{TL}$  and  $\Delta IWC^{TL}$  as a function of  $\delta t^{TL}$  (as demonstrated in section 4.1). Over MariCont-O, ice injection in the TL is longer than over IndOc and PacOc ( $\Delta t^{TL} = 8-11, 6-9$  and  $6-9$  h, respectively). The amount of ice injected over MariCont-O is greater than over IndOc and PacOc ( $\Delta IWC^{TL} = 0.16-0.19, 0.09-0.10, 0.08-0.09$  mg m<sup>-3</sup>, respectively). Furthermore, the ice background in the TL is also greater over MariCont-O than over IndOc and PacOc  
575 ( $IWC_{min}^{TL} \sim 0.34-0.37, 0.24-0.26, 0.29-0.30$  mg m<sup>-3</sup>, respectively). Thus, while the diurnal cycle of Prec over MariCont-O is the weakest, the diurnal cycle of ice over MariCont-O would have the highest values.

As expected from the SMILES measurements, the MariCont region presents the largest ice injection in the TL. While the IWC background over MariCont-O is the largest, the injection of IWC over MariCont-L is the most important. Furthermore,

all these results are consistent with the OLR from the NOAA, showing strongest values over region having OLR signal such as over lands (not shown).

580

## 5. Discussion on the processes driving the decreasing phase of the IWC diurnal cycle

The previous section has shown that the growing phase of the diurnal cycle of deep convection in the tropics impacts on the growing phase of diurnal cycle of ice in the UT and the TL. In this section, the convective processes impacting the decreasing phase of the ice diurnal cycle in the UT and the TL are discussed. The decreasing phase of the diurnal cycle of ice in the UT and the TL represents the diurnal loss of ice. This loss can be caused by several processes including sedimentation, downdraft convective processes during the dissipating stage, sublimation into water vapour or horizontal advection and mixing. Quantifying the processes impacting the diurnal cycle of ice can help to quantify the amount of water staying into the UT and TL, the part falling down to the surface and the part advected up to the LS at the temporal diurnal scale.

585

In this section, the comparison between the value of IWC measured by MLS during the decreasing phase ( $IWC_x$ ) at ( $x = \text{Day or Night}$ ) and IWC estimated at the same  $t_x$  ( $IWC(t_x)$ ) is discussed. If  $IWC_x \sim IWC(t_x)$ , our model based on Prec evolution is a good predictive tools to consider that convective processes (as represented by Prec) control the decreasing phase of the ice diurnal cycle. Otherwise, non-convective processes has also need to be investigated to explain the ice diurnal cycle. Table 5 presents the difference  $d$  ( $d = IWC(t_x) - IWC_x$ ) in the UT and the TL.

590

595

Over land in the UT,  $d$  is positive and less than 23 % over SouthAm and SouthAfr and close to zero over the MariCont-L. The fact that the amount of Prec over SouthAm and SouthAfr is greater than required to explain IWC suggests that a significant fraction of the convection is shallow and does not reach the UT. In contrast, over the MariCont-L, the diurnal cycle of Prec is very similar to the diurnal cycle of IWC suggesting that the convective activity over this region brings a large amount of ice all over the 24 hours. In the TL,  $d$  is found between -14 and -20 % implying that the ice decreases more slowly than Prec.

600

Over ocean in the UT,  $d$  is negative down to -26 % showing that the ice stay longer in the UT compared to the Prec decreasing phase. In the TL,  $d$  varies between +9 and -7 showing low differences  $d$  at this level.

In summary, the method presented in the present paper allows to estimate the diurnal cycle of ice in the UT and the TL to within 26 % over the 6 tropical zones and to within 14 % over the MariCont-L region.

## 6. Conclusion and perspectives

To quantify the amount of ice injected in tropical upper troposphere (UT) and the tropopause layer (TL) and the processes linked to the ice diurnal variation is important to better understand the amount of total water in these layers and the amount of water entering into the LS. The information given by MLS on the diurnal cycle of ice water content (IWC) in the UT and the TL and the method comparing the two per day measurements (Liu and zipser, 2005 and Carminati et al., 2014) are too limited to estimate the ice variability in these layers. Thus, the present study starts to assume that the diurnal cycle in ice is related to the diurnal cycle in precipitation (for which there are TRMM data with much better time resolution) in austral

610

convective tropics. The high relationship between precipitation (Prec) measured by TRMM and IWC measured by MLS in the UT and the TL is shown in the study. As MLS measures IWC only twice a day, at 01:30 (Night) and 13:30 LT (Day), we  
615 have proposed a simple model based on the diurnal cycle of Prec to estimate the diurnal cycle of IWC in the UT and in the TL. The method is validated using the short period of DJF 2009-2010 of ice measurement from the SMILES instrument in the troposphere and the TL.

Because of the strong space correlation between Prec and IWC, we show that Prec can be used as a proxy of the deep convection reaching the UT and the TL during the growing stage of the convection in order to bring ice in the UT and the  
620 TL. The method proposed in the study allows to estimate 1) the diurnal cycle of ice into the UT and the TL and 2) the difference between the maximum and the minimum in the diurnal cycle of ice in these layers, namely the amount of ice injected by deep convection. Our method suggests that deep convection is the most important process in austral convective tropics driving the diurnal increase of ice in these layers. Other processes may play a minor role such as the decrease of the temperature in the TTL, increasing the saturation ratio and allowing the crystal nucleation and growth, or the **transport** of ice  
625 in the UT and TL by horizontal advection.

The amount of ice injected in the UT ( $2.73 \text{ mg m}^{-3}$  over land and  $0.60 \text{ mg m}^{-3}$  over ocean) is found to be much higher than the amount of ice injected in the TL ( $0.26\text{-}0.41 \text{ mg m}^{-3}$  over land and  $0.11\text{-}0.13 \text{ mg m}^{-3}$  over ocean). Furthermore, the study highlights the importance to separate the land of the Maritime Continent (MariCont-L) to the ocean of the Maritime  
630 Continent (MariCont-O) to better understand the ice diurnal cycle in the UT and the TL over the complex and strong convective region of the Maritime Continent. It has been shown that the injection of ice over the MariCont-L into the UT and the TL ( $\Delta IWC^{UT} = 3.34 \text{ mg m}^{-3}$ ,  $\Delta IWC^{TL} = 0.56\text{-}0.42 \text{ mg m}^{-3}$ ) is the greatest in the tropics. **This injection of ice would have a strong importance on the amount of ice entering into the LS and feeding what has been called the 'stratospheric fountain' (Newell and Gould-Stewart, 1981) observed over the MarCont region.**

The decreasing phase of the ice diurnal cycle is also evaluated with Prec and discussed. While, **it is difficult to quantify the impact of other processes than convective processes on the diurnal cycle of ice in the UT and the TL, we are able to assess that the deep convection impacts on the depletion of ice during the decreasing phase of the ice diurnal cycle (from Table 5: 97 % in the UT over the MariCont and ~80 % in averaged UT and TL over other regions).** Thus, Prec is also considered to be a good proxy of the decreasing phase of the convection, especially over the MariCont-L region in the UT (to within 3 %, according to Table 5), and **convective processes are the main processes impacting the decreasing phase of the diurnal cycle**  
640 **of ice.** Furthermore, our study has shown that the estimated diurnal variation of ice is the largest in the regions (identified from TRMM) where the diurnal variation in temperature is also the largest although horizontal transport may play a role, but **it cannot be quantified using our methodology.**

In summary, **while the importance of deep convective processes and large-scale three-dimensional circulation processes on the ice and water injection up to the UT, TL and LS are still debated, this study shows that** the ice diurnal cycle in the UT and  
645 the TL is mainly governed by vertical processes linked to the convective activity that are much stronger than other processes such as **e.g. horizontal mixing, sublimation, sedimentation,...**

Although it is beyond the scope of the present paper, some potentially new results might be achievable using our method as e.g. the part of ice sublimating during deep convection, the impact of intra-seasonal variability such as ENSO and the Madden Jullian Oscillation (MJO) on the ice diurnal cycle. In fact, ENSO and MJO have a strong influence on the tropical  
650 deep convection and injection of moisture into the TTL (Gettelman et al., 2002; Wong and Dessler, 2007) and are associated to the cold anomalies near the TTL, especially over the Maritime Continent region (Zhang et al., 2013). We are expecting a strong impact on the diurnal ice injection timing and duration in the TL. The processes impacting the ice injection into the UT and the TL over the Maritime Continent regions at local scale will be studied in a forthcoming paper.

## 655 **Acknowledgment**

Our study takes place within the Turbulence Effects on Active Species in Atmosphere (TEASAO – <http://www.legos.obs-mip.fr/projets/axes-transverses-processus/teasao>) project. We thank the National Center for Scientific Research (CNRS) and the Excellence Initiative (Idex) of Toulouse, France (TEASAO project, Peter Haynes Chair of Attractivy) to fund this study. We would like to thank the teams that have provided the MLS data ([https://disc.gsfc.nasa.gov/datasets/ML2IWC\\_V004](https://disc.gsfc.nasa.gov/datasets/ML2IWC_V004)), the  
660 TRMM data (<https://pmm.nasa.gov/data-access/downloads/trmm>) and the SMILES data (<https://mls.jpl.nasa.gov/data/smiles>).

## **References**

- 665 Alcalá, Dessler, A. E.: Observations of deep convection in the tropics using the Tropical Rainfall Measuring Mission (TRMM) precipitation radar, *J. of Geo. Res.*, vol. 107, NO. D24, 4792, doi:10.1029/2002JD002457, 2002.
- Allison, T., Fuelberg, H., Heath, N.: Simulations of Vertical Water Vapor Transport for TC Ingrid (2013). *J. of Geophys. Res.: Atmospheres*, 123(15), 8255-5282, doi: 10.1029/2018JD028334, 2018.
- Avery, M. A., Davis, S. M., Rosenlof, K. H., Ye, H. and Dessler, A. E.: Large anomalies in lower stratospheric water vapour  
670 and ice during the 2015-2016 El Nino, *Nat. Geosci.*, 10(6), 405–409, doi:10.1038/ngeo2961, 2017.
- Beucher, F.: Manuel de météorologie tropicale: des alizés au cyclone tropical, Météo-France, Paris, France, 2010.
- Birner, T. and Charlesworth, E. J.: On the relative importance of radiative and dynamical heating for tropical tropopause temperatures, *J. Geophys. Res. Atmospheres*, 122(13), 6782-6787, doi:10.1002/2016JD026445, 2017.
- Carminati, F., Ricaud, P., Pommereau, J.-P., Rivière, E., Khaykin, S., Attié, J.-L., and Warner, J.: Impact of tropical land  
675 convection on the water vapour budget in the tropical tropopause layer, *Atmos. Chem. Phys.*, 14, 6195-6211, doi:10.5194/acp-14-6195-2014, 2014.
- Corti, T., Luo, B. P., Fu, Q., Vömel, H. & Peter, T.: The impact of cirrus clouds on tropical troposphere-to-stratosphere transport. *Atmos. Chem. and Phys.* 6, 2539–2547, doi:10.5194/acp-6-2539-2006, 2006.
- Corti T, Luo BP, Reus M de, Brunner D, Cairo F, Mahoney MJ: Unprecedented evidence for deep convection hydrating the  
680 tropical stratosphere. *Geophys. Res. Letters.*, 35(10), doi:10.1029/2018GL033641, 2008.

- Dauhut, T., Chaboureau, J.-P., Escobar, J., Mascart, P.: Large-eddy simulations of Hector the convective making the stratosphere wetter. *Atmos. Sci. Letters* 16, 135–140., doi:10.1002/asl2.534, 2015.
- 685 Fahey, D. W., Kelly, K. K., Ferry, G. V., Poole, L. R., Wilson, J. C., Murphy, D. M., Loewenstein, M., and Chan, K. R.: In situ measurements of total reactive nitrogen, total water, and aerosol in a polar stratospheric cloud in the Antarctic. *J. Geophys. Res.* 94, 11299–11315, doi:10.1029/JD094iD09p11299, 1989.
- Fueglistaler, S., Dessler, A. E., Dunkerton, T. J., Folkins, I., Fu, Q. and Mote, P. W.: Tropical tropopause layer, *Rev. Geophys.*, 47(1), RG1004, doi:10.1029/2008RG000267, 2009.
- 690 Gettelman, A. and Forster, P. M. de F.: A Climatology of the Tropical Tropopause Layer, *J. Meteorol. Soc. Jpn. Ser II*, 80(4B), 911–924, doi:10.2151/jmsj.80.911, 2002.
- Hartmann, D. L., Holton, J. R., Fu, Q.: The heat balance of the tropical tropopause, cirrus, and stratospheric dehydration. *Geo. Res. Letters* 28, 1969–1972, 2001.
- Hegglin, M. I., Plummer, D. A., Shepherd, T. G., Seinoeca, J.F., Anderson, J., Froidevaux, L., Funke, B., Hurst, D., Rozanov, A., Urban, J., von Clarmann, T., Walker, K. A., Wang, H. J., Tegtmeier, S., Weigel, K.: Vertical structure of stratospheric water vapour trends derived from merged satellite data. *Nature Geoscience*, 7, 768–776, doi: 10.1038/ngeo2236, 2014.
- 695 Holton, J. R., Haynes, P. H., McIntyre, M. E., Douglass, A. R., Rood, R. B., Pfister, L.: Stratosphere-troposphere exchange. *Rev. Geophys.* 33, 403–439. doi: 10.1029/95RG02097, 1995.
- Holton, J. R. and Gettelman, A.: Horizontal transport and the dehydration of the stratosphere, *Geophys Res Lett*, 28(14), 2799–2802, doi: 10.1029/2001GL013148, 2001.
- Jensen, E. J., Toon, O. B., Pfister, L., Selkirk, H. B.: Dehydration of the upper troposphere and lower stratosphere by subvisible cirrus clouds near the tropical tropopause, *Geophys Res Lett*, doi: 10.1029/96GL00722, 1996.
- Jensen, E. J., Smith, J. B., Pfister, L., Pittman, J. V., Weinstock, E. M., Sayres, D. S., ... Wilson, J. C. (2005). Ice supersaturations exceeding 100% at the cold tropical tropopause: implications for cirrus formation and dehydration. *Atmospheric Chemistry and Physics*, 5(3), 851–862, doi: 10.5194/acp-5-851-2005, 2005.
- 705 Jensen, E. J.: Physical processes controlling ice concentrations in synoptically forced, midlatitude cirrus. *J. of Geophys. Res.: Atmospheres*, 118(11), 5348–5360, doi: 10.1002/jgrd.50421, 2013.
- Jiang, J. H., Su, H., Zhai, C., Janice Shen, T., Wu, T., Zhang, J., et al.: Evaluating the Diurnal Cycle of Upper-Tropospheric Ice Clouds in Climate Models Using SMILES Observations. *J. Atmos. Sci.* 72, 1022–1044., doi:10.1175/JAS-D-14-0124.1, 2014.
- 710 Khaykin, S., Pommereau, J.-P., Korshunov, L., Yushkov, V., Nielsen, J., Larsen, N., Christensen, T., Garnier, A., Lukyanov, A., and Williams, E.: Hydration of the lower stratosphere by ice crystal geysers over land convective systems, *Atmos. Chem. Phys.*, 9, 2275–2287, doi: 10.5197/acp-9-2275-200, 2009.
- Khaykin, S. Mk., J.-P. Pommereau and A. Hauchecorne: Impact of land convection on temperature diurnal variation in the

- 715 tropical lower stratosphere inferred from COSMIC GPS radio occultations, *Atmos. Chem. Phys.*, 13, 6391-6402, doi: 10.5194/acp-13-6391-2013, 2013.
- Khaykin, S. M., Pommereau, J.-P., Riviere, E. D., Held, G., Ploeger, F., Ghysels, M., Armarouche, N., Vernier, J.-P., Wienhold, F., G., Ionov, D.: Evidence of horizontal and vertical transport of water in the Southern Hemisphere tropical tropopause layer (TTL) from high-resolution balloon observations. *Atmospheric Chemistry and Physics* 16, 12273–12286, doi: 10.5194/acp-16-12273-2016, 2016.
- 720 Kim, J. and Son, S.-W. Tropical Cold-Point Tropopause: Climatology, Seasonal Cycle, and Intraseasonal Variability Derived from COSMIC GPS Radio Occultation Measurements. *J. Climate*, 25, 5343–5360, doi: 10.1175/JCLI-D-11-00554.1, 2012.
- Liu, C. and Zipser, E. J.: Global distribution of convection penetrating the tropical tropopause, *J. Geophys. Res. Atmospheres*, 110(D23), D23104, doi:10.1029/2005JD006063, 2005.
- 725 Livesey, N. J., Read, W. G. and Wagner, P. A.: Version 4.2x Level 2 data quality and description document, 2017.
- Maycock, A. C., Joshi, M. M., Shine, K. P. and Scaife, A. A.: The Circulation Response to Idealized Changes in Stratospheric Water vapour, *J. Clim.*, 26(2), 545–561, doi:10.1175/JCLI-D-12-00155.1, 2012.
- Mehta, S. K., Krishna Murthy, B. V., Narayana Rao, D., Venkat Ratnam, M., Parameswaran, K., Rajeev, K., Suresh Raju, C., Kusuma, G. Rao.: Identification of tropical convective tropopause and its association with cold point tropopause. *J. Geophys. Res.* 113, D00B04, doi: 10.1029/2007JD009625, 2008.
- 730 Millán, L., Read, W., Kasai, Y., Lambert, A., Livesey, N., Mendrok, J., Sagawa, H., Sano, T., Shiotani, M. and Wu, D. L.: SMILES ice cloud products, *J. Geophys. Res. Atmospheres*, 118(12), 6468–6477, doi:10.1002/jgrd.50322, 2013.
- Mote, P. W. et al.: An atmospheric tape recorder: The imprint of tropical tropopause temperatures on stratospheric water vapour. *J. Geophys. Res.* 101, 3989–4006, doi: 0148-0227/96/95JD-03422 \$05.00, 1996.
- 735 Nesbitt, S. W., Zipser, E. J., Cecil, D. J.: A Census of Precipitation Features in the Tropics Using TRMM: Radar, Ice Scattering, and Lightning Observations. *J. Climate* 13, 4087–4106, doi: 10.1175/1520-0442(2000)013<4087:ACOPFI>2.0.CO;2, 2000.
- Stenke, A. and Grewe, V.: Simulation of stratospheric water vapor trends: impact on stratospheric ozone chemistry, *Atmos. Chem. Phys.*, 5, 1257-1272, doi: 10.5194/acp-5-1257-2005, 2005.
- 740 Newell, R. E. and Gould-Stewart, S.: A Stratospheric Fountain?, *J. Atmospheric Sci.*, 38(12), 2789–2796, doi:10.1175/1520-0469(1981)038<2789:ASF>2.0.CO;2, 1981.
- Pereira, L. G., Rutledge, S. A.: Diurnal Cycle of Shallow and Deep Convection for a Tropical Land and an Ocean Environment and Its Relationship to Synoptic Wind Regimes. *Mon. Wea. Rev.* 134, 2688–2701, doi: 10.1175/MWR3181.1, 2006.
- 745 Peter, T. et al.: When Dry Air Is Too Humid. *Science* 314, 1399–1402., 2006.
- Petersen, W. A., Rutledge, S. A.: Regional Variability in Tropical Convection: Observations from TRMM. *J. Climate* 14, 3566–3586, doi: 10.1175/1520-0442(2001)014<3566:RVITCO>2.0.CO;2, 2001.
- Pommereau, J.-P.: Troposphere-to-stratosphere transport in the tropics. *Comptes Rendus Geoscience* 342, 331–338., doi:

10.1016/j.crte.2009.10.015, 2010.

- 750 Potter, B. E., and J. R. Holton: The role of monsoon convection in the dehydration of the lower tropical stratosphere, *J. Atmos. Sci.*, 38, 1034–1050, doi: 10.1175/1520-0469(1995)052<1034:TROMCI>2.0.CO;2, 1995.
- Ricaud, P. et al. Equatorial total column of nitrous oxide as measured by IASI on MetOp-A: implications for transport processes. *Atmos. Chem. Phys.* 9, 3947–3956, doi: 10.5194/acp-9-3947-2009, 2009.
- Schoeberl, M. R., Jensen, E. J., Pfister, L., Ueyama, R., Avery, M., and Dessler, A. E.: Convective hydration of the upper  
755 troposphere and lower strato- sphere. *Journal of Geophysical Research: Atmospheres*, 123, 4583–4593., doi:10.1029/2018JD028286, 2018.
- Sherwood, S. C. and Dessler, A. E.: On the control of stratospheric humidity, *Geophys. Res. Lett.*, 27(16), 2513–2516, doi:10.1029/2000GL011438, 2000.
- Solomon, S. Stratospheric ozone depletion: A review of concepts and history. *Rev. Geophys.* 37, 275–316, doi:  
760 10.1029/1999RG900008, 1999.
- Solomon, S. et al. Contributions of Stratospheric Water Vapor to Decadal Changes in the Rate of Global Warming. *Science* 327, 1219–1223, doi: 10.1029/1999RG900008, 2010.
- Suneeth, K. V., Das, S. S. and Das, S. K.: Diurnal variability of the global tropical tropopause: results inferred from COSMIC observations, *Clim. Dyn.*, doi:10.1007/s00382-016-3512-x, 2017.
- 765 Takahashi, H., Luo, Z. J. Characterizing tropical overshooting deep convection from joint analysis of CloudSat and geostationary satellite observations. *Journal of Geophysical Research: Atmospheres* 119, 112–121, doi: 10.1002/2013JD020972, 2014.
- TRMM. Available at: [https://trmm.gsfc.nasa.gov/publications\\_dir/publications.html](https://trmm.gsfc.nasa.gov/publications_dir/publications.html).
- Ueyama, R., Jensen, E. J., Pfister, L. and Kim, J.-E.: Dynamical, convective, and microphysical control on wintertime  
770 distributions of water vapour and clouds in the tropical tropopause layer, *J. Geophys. Res. Atmospheres*, 120(19), 2015JD023318, doi:10.1002/2015JD023318, 2015.
- Vogel, B., Feek, T., and Groß, J.-U.: Impact of stratospheric water vapor enhancements caused by CH<sub>4</sub> and H<sub>2</sub> increase on polar ozone loss, *J. Geophys. Res.*, 116, D05301, doi: 10.1029/2010JD014234, 2011.
- 775 Wright, J. S., Fu, R., Fueglistaler, S., Liu, Y. S., and Zhang, Y.: The influence of summertime convection over Southeast Asia on water vapor in the tropical stratosphere, *J. Geophys. Res.*, 116, D12302, doi:10.1029/2010JD015416, 2011.
- Wong, S., and Dessler, A., E.: Regulation of H<sub>2</sub>O and CO in tropical tropopause layer by the Madden-Julian oscillation, *J. Geophys. Res.*, 112, D14305, doi:10.1029/2006JD007940, 2007.
- Yang, G.-Y. and Slingo, J.: The diurnal cycle in the tropics, *Mon. Weather Rev.*, 129(4), 784–801, doi: 10.1175/1520-0493(2001)129<0784:TDCITT>2.0.CO;2, 2001.
- 780 Zhang, C.: Madden–Julian Oscillation: Bridging Weather and Climate. *Bull. Amer. Meteor. Soc.* 94, 1849–1870, doi:10.1175/BAMS-D-12-00026.1, 2013.

Zhou, C., Dessler, A. E., Zelinka, M. D., Yang, P., and Wang, T.: Cirrus feedback on interannual climate fluctuations, *Geophys. Res. Lett.*, 41, 9166–9173, doi:10.1002/2014GL062095., 2014.

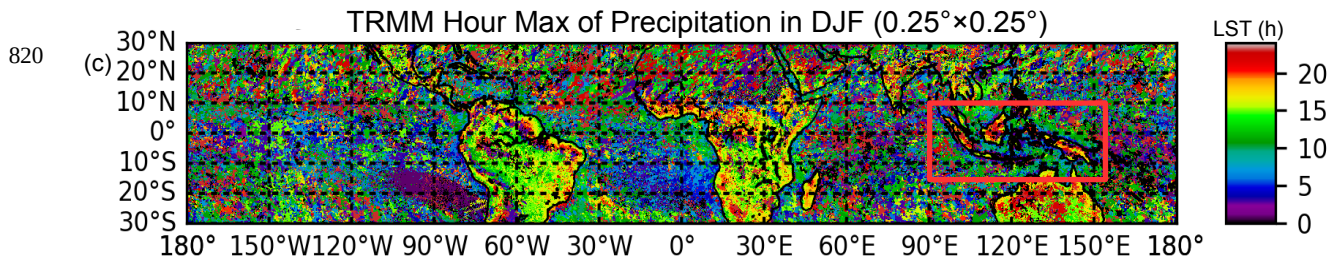
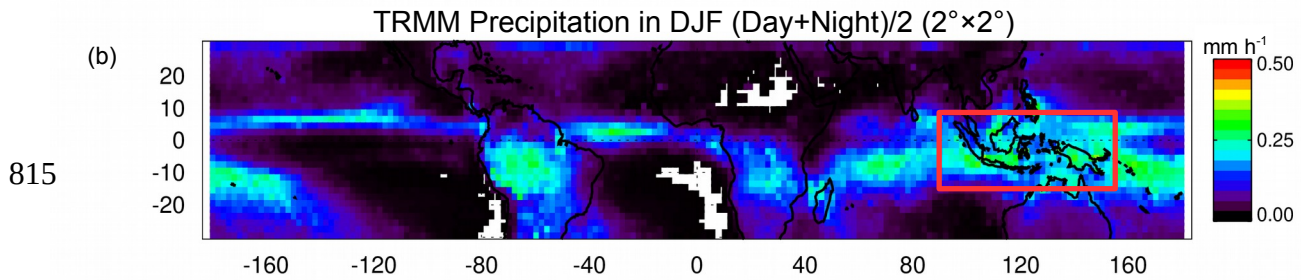
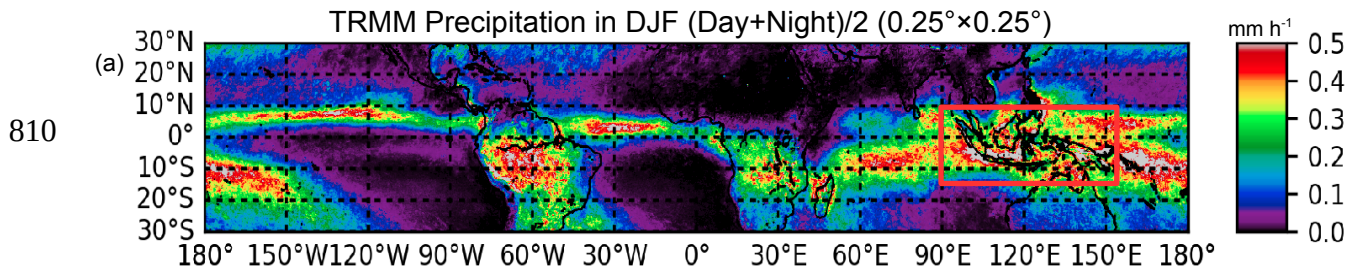
785

790

795

800

805

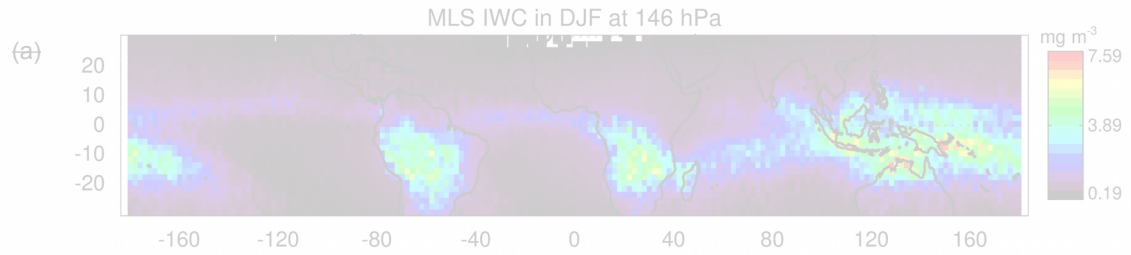


825

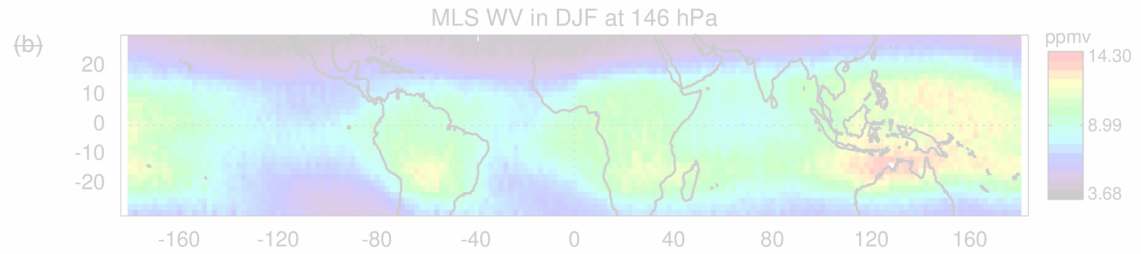
**Figure 1: (From top to bottom): (a) (Day+Night)/2 of precipitation measured by TRMM at  $0.25^\circ \times 0.25^\circ$  resolution (mm/h), (b) (Day+Night)/2 of precipitation at  $2^\circ \times 2^\circ$  resolution (mm/h), and (c) hour of diurnal maximum of precipitation at  $0.25^\circ \times 0.25^\circ$  resolution (h in Local Solar Time, LST) in DJF over the period 2004-2017. The red box surrounds the MariCont region.**

830

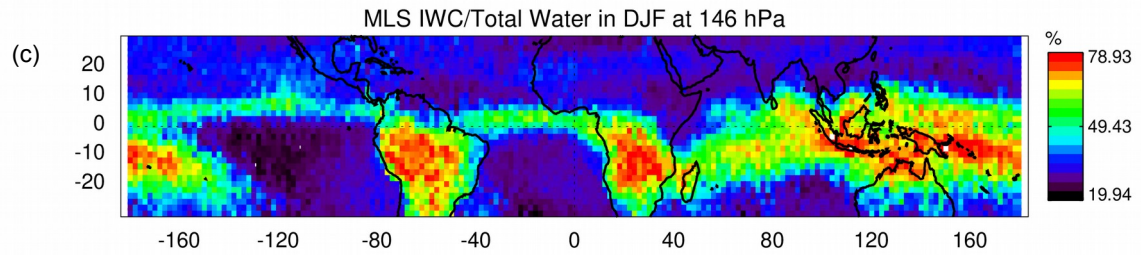
835



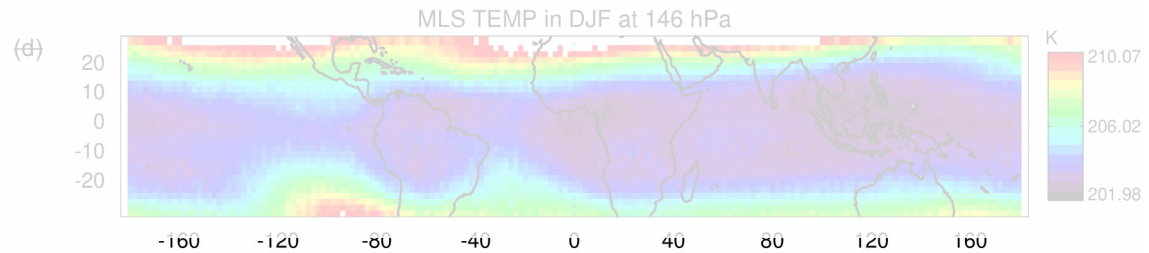
840



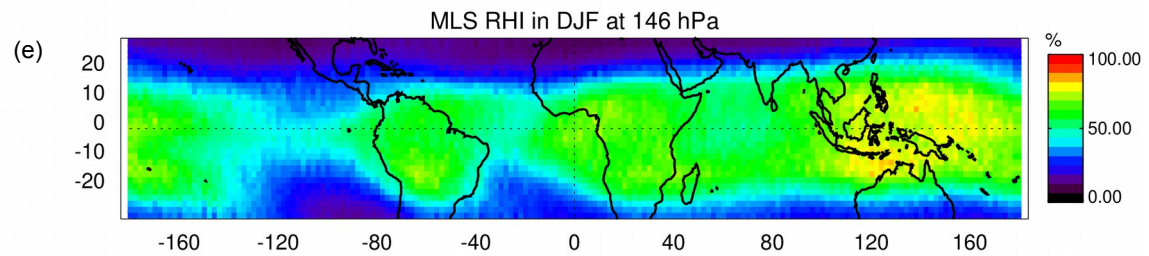
845



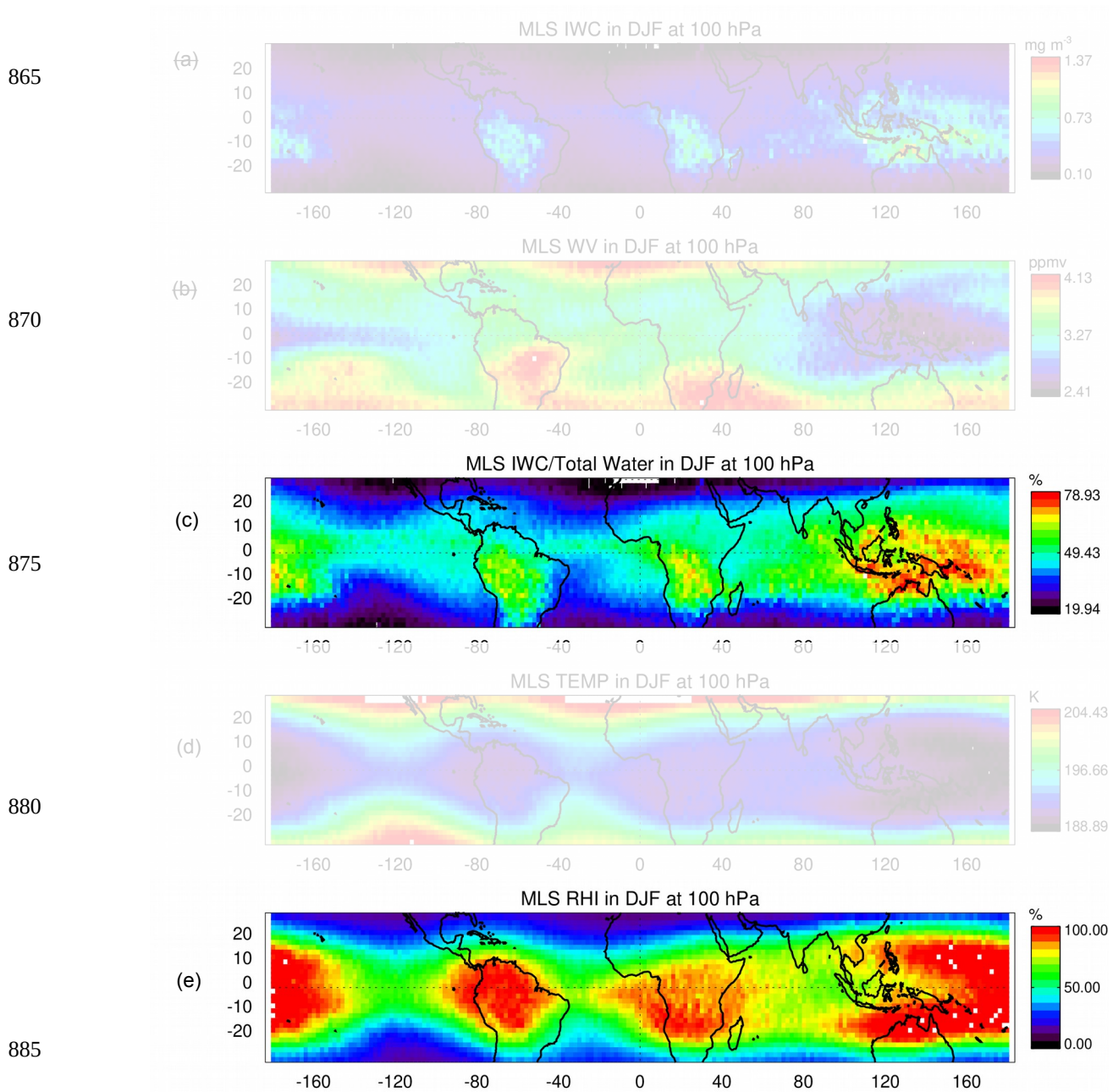
850



855



860 **Figure 2:** (From top to bottom): (a) daily average (Day+Night)/2 of Ice Water Content (IWC), (b) Water Vapour (WV), (c) IWC fraction (IWC/ $\Sigma$ W), (d) Temperature and (e) Relative Humidity with respect to Ice (RHI) in the upper troposphere (146 hPa) measured by MLS over the tropics in DJF over the period 2004-2017.



890 **Figure 3** - (From top to bottom): (a) daily average (Day+Night)/2 of Ice Water Content (IWC), (b) Water Vapour (WV), (c) IWC fraction ( $IWC/\Sigma W$ ), (d) Temperature and (e) Relative Humidity with respect to Ice (RHI) in the tropopause layer (100 hPa) measured by MLS over the tropics in DJF over the period 2004-2017.

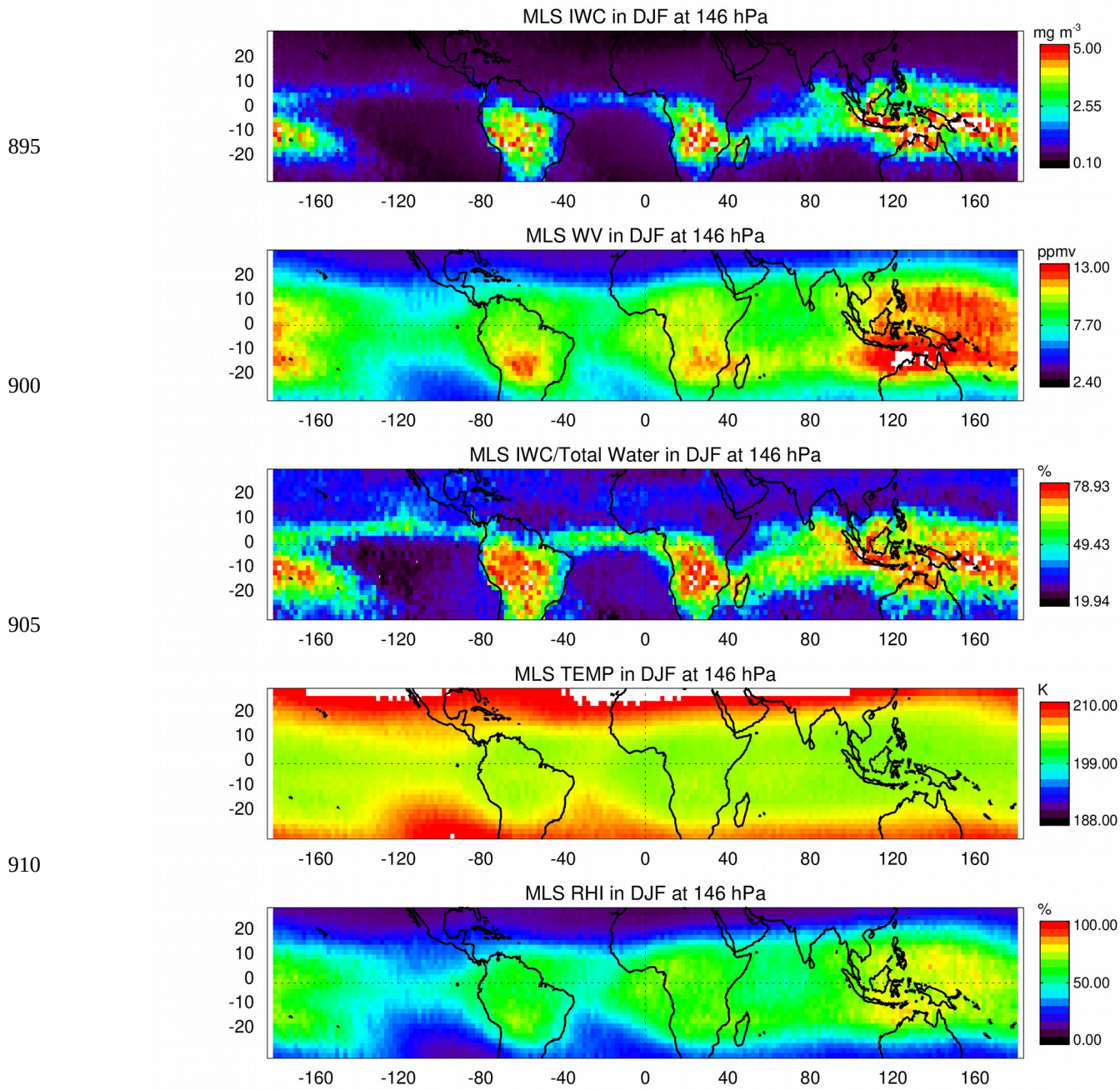
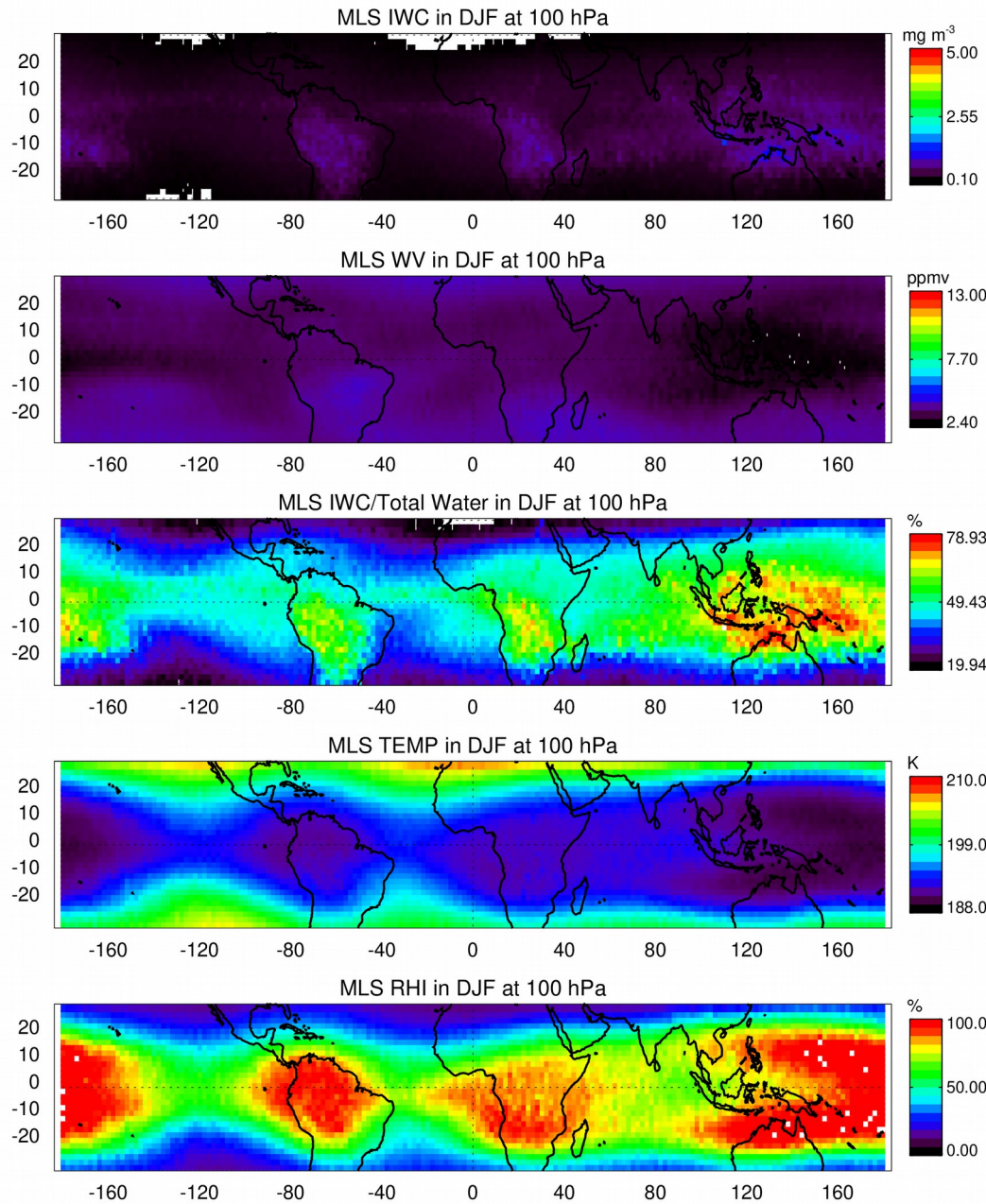


**Figure 2:** (From top to bottom): (a) daily average (Day+Night)/2 of Ice Water Content (IWC), (b) Water Vapour (WV), (c) IWC fraction (IWC/ $\Sigma$ W), (d) Temperature and (e) Relative Humidity with respect to Ice (RHI) in the upper troposphere (146 hPa) measured by MLS over the tropics in DJF over the period 2004-2017.

920



925

930

935

940

945 **Figure 3:** (From top to bottom): (a) daily average (Day+Night)/2 of Ice Water Content (IWC), (b) Water Vapour (WV), (c) IWC fraction ( $\text{IWC}/\Sigma\text{W}$ ), (d) Temperature and (e) Relative Humidity with respect to Ice (RHI) in the tropopause layer (100 hPa) measured by MLS over the tropics in DJF over the period 2004-2017.

950

955

960

965

970

975

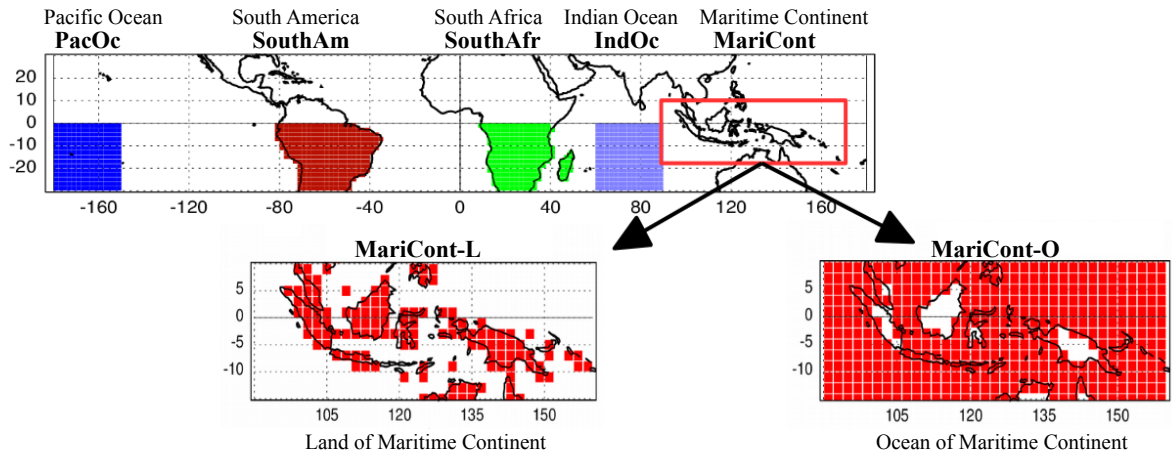
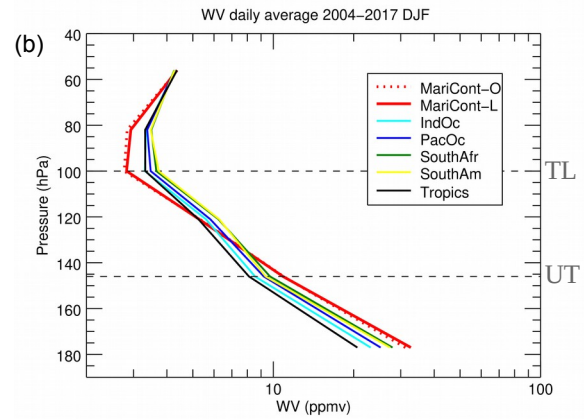
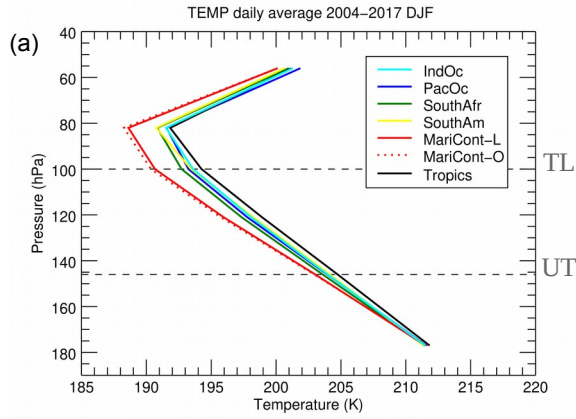
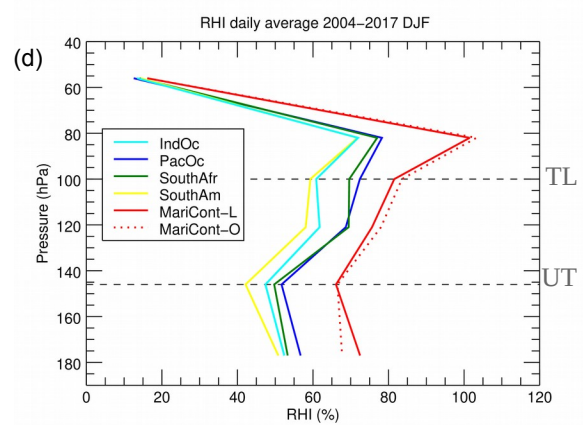
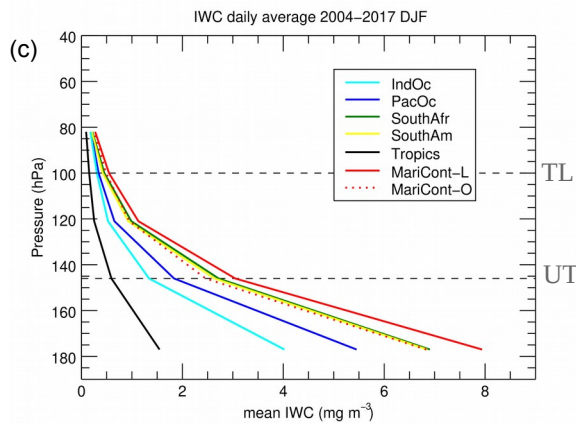


**Figure 2: Representation of the study zones: PacOc, Pacific Ocean; SouthAm, South America; SouthAfr, South Africa; IndOc, Indian Ocean; MariCont-L, land of the Maritime Continent; MariCont-O, ocean of the Maritime Continent. Each zone is defined at a horizontal resolution of  $2^\circ \times 2^\circ$ .**

980



985



990

**Figure 3: Vertical profiles of (a) temperature, (b) Water Vapour (WV), (c) Ice Water Content (IWC) and (d) Relative Humidity with respect to Ice (RHI) from MLS data averaged from 2004 to 2017 in DJF over the 6 study zones: IndOc (light blue), PacOc (dark blue), SouthAfr (green), SouthAm (yellow), Tropics (black), MariCont-L (red solid line) and MariCont-O (red dashed line).**

995

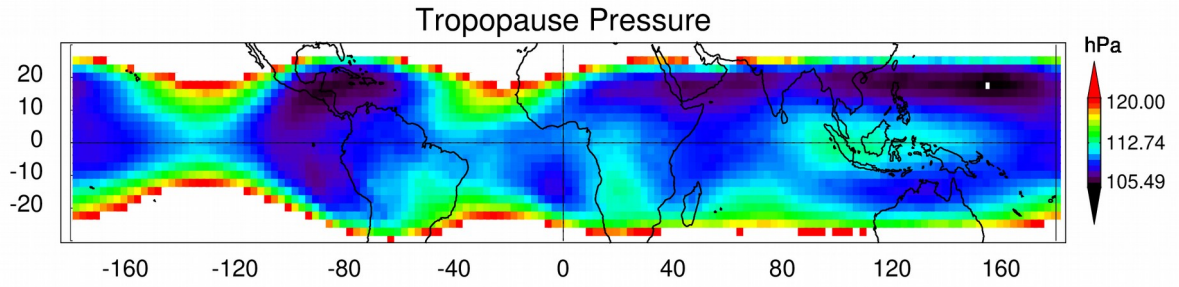
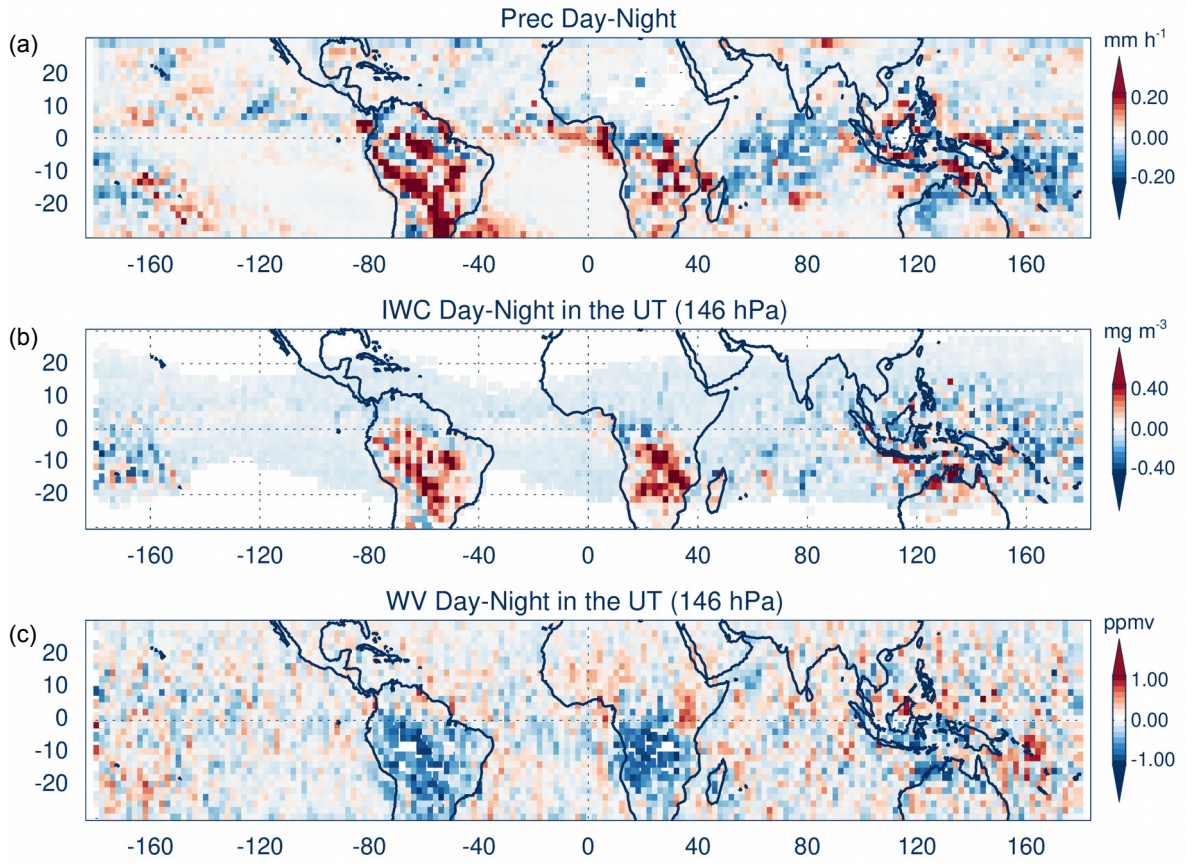


**Figure 4: Pressure of the tropopause (hPa) over the tropics during DJF from 2004 to 2017, defined from the NCEP datasets.**

1005

1010

1015



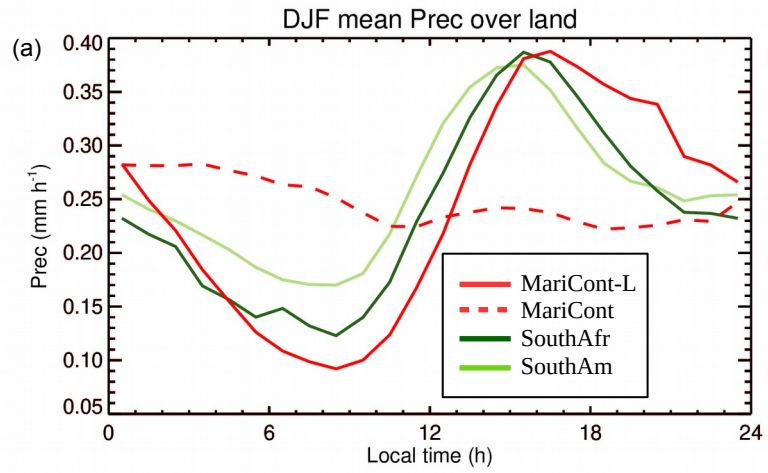
1020

1025

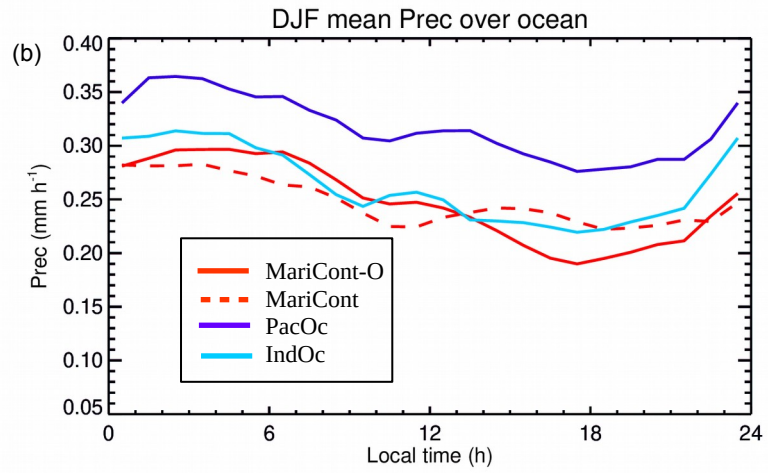
1030 **Figure 5: Day–Night of (a) precipitation (Prec) from TRMM, (b) Ice Water Content (IWC) from MLS at 146 hPa and (c) Water Vapour (WV) from MLS at 146 hPa over the tropics and the period 2004-2017 in DJF.**

1035

1040



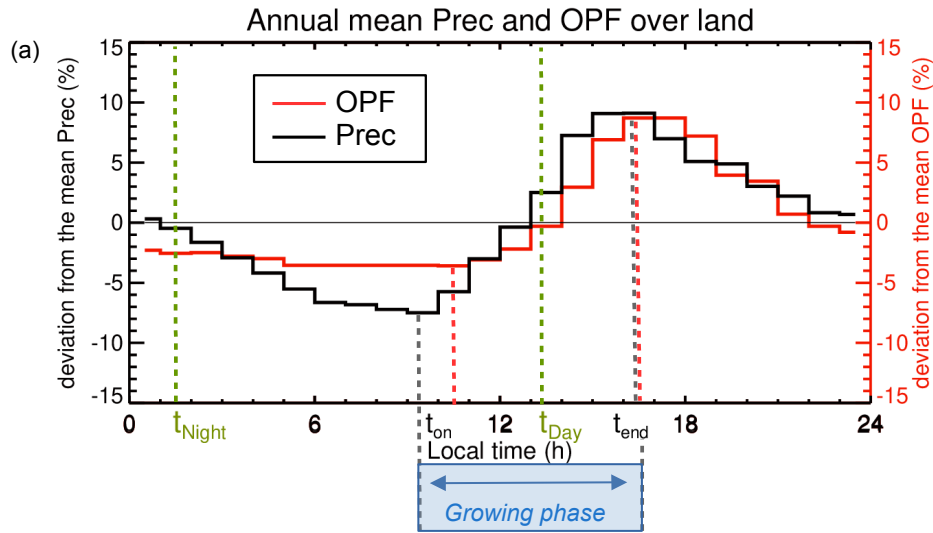
1045



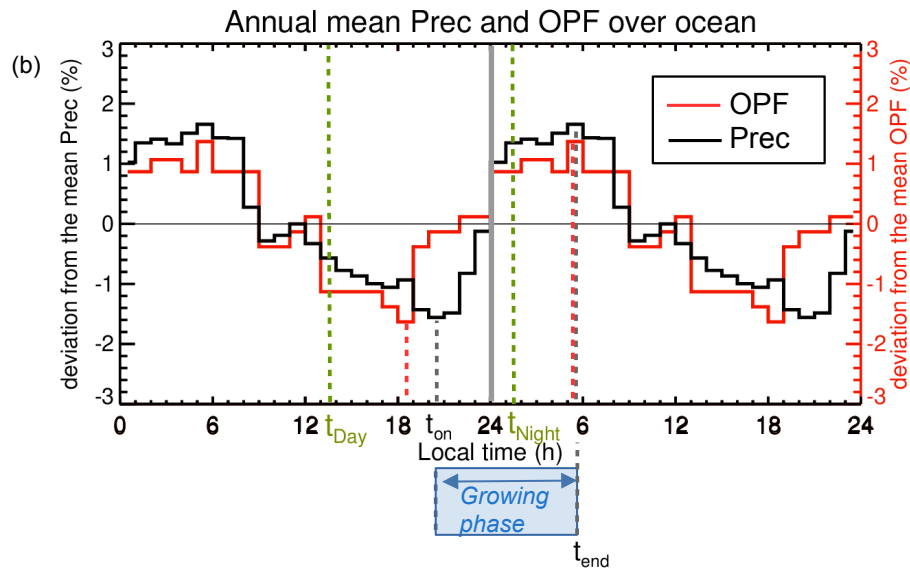
1050

**Figure 6: Diurnal cycle of precipitation (Prec) over (a) the land study zones and (b) the ocean study zones during the period DJF 2004-2017.**

1055



1060



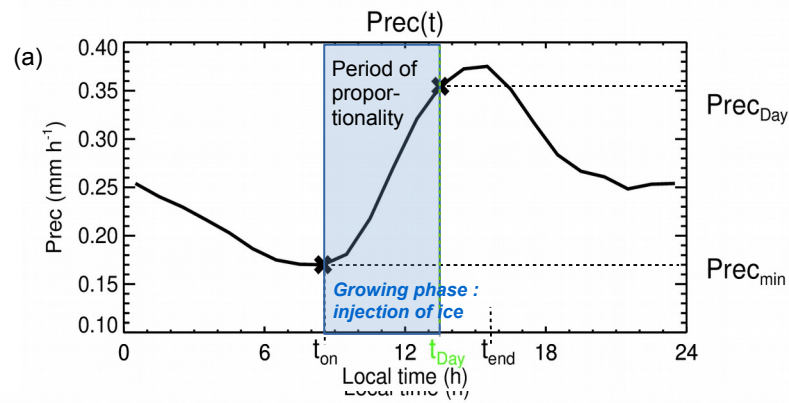
1065

1070

Figure 7: (Top) Deviation from the mean of the annual mean diurnal cycle of TRMM precipitation (Prec, in black solid line) over land, from 2004 to 2017 and diurnal cycle of overshooting precipitation features (OPFs) at the tropopause (red solid line) over land, from 1998 to 2000 and from 2001 to 2003 adapted from Liu and Zipser (2005) over the tropics ( $20^{\circ}\text{N}$ - $20^{\circ}\text{S}$ ). (Bottom) Same as top but over the ocean. Minimum and maximum of Prec and OPF are drawn with vertical dotted lines (in black and red, respectively).  $t_{on}$  is the time of the onset of the Prec,  $t_{end}$  is the time of the diurnal maximum of Prec,  $t_{Day}$  and  $t_{Night}$  are the times of the two MLS measurements at Day and Night, respectively.

1075

1080



1085

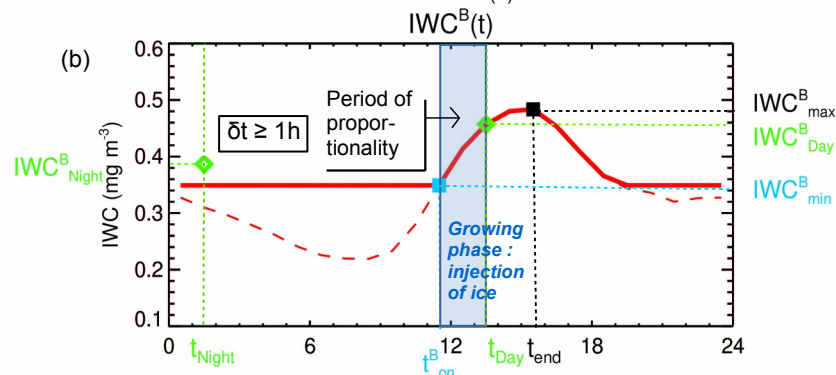
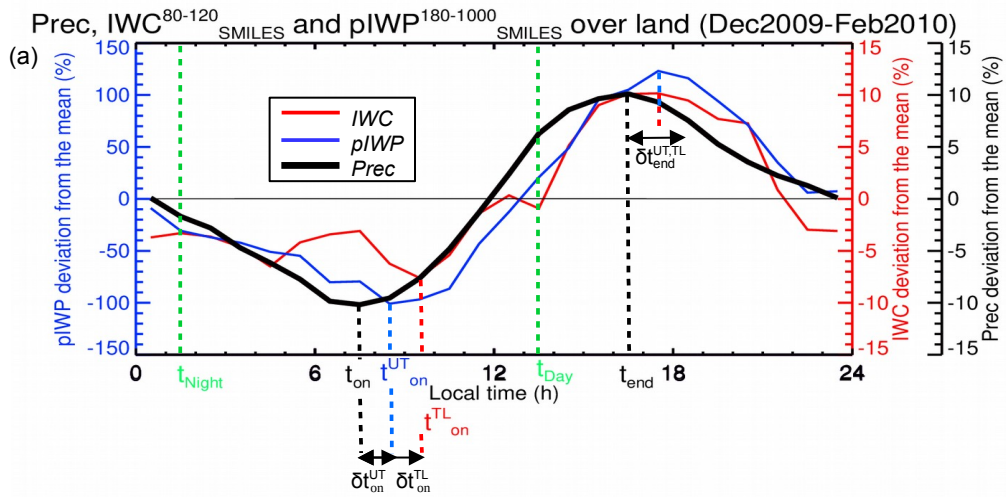


Figure 8: Methodology to estimate the diurnal cycle of ice water content (IWC) over land: (a) diurnal cycle of precipitation, with

1090

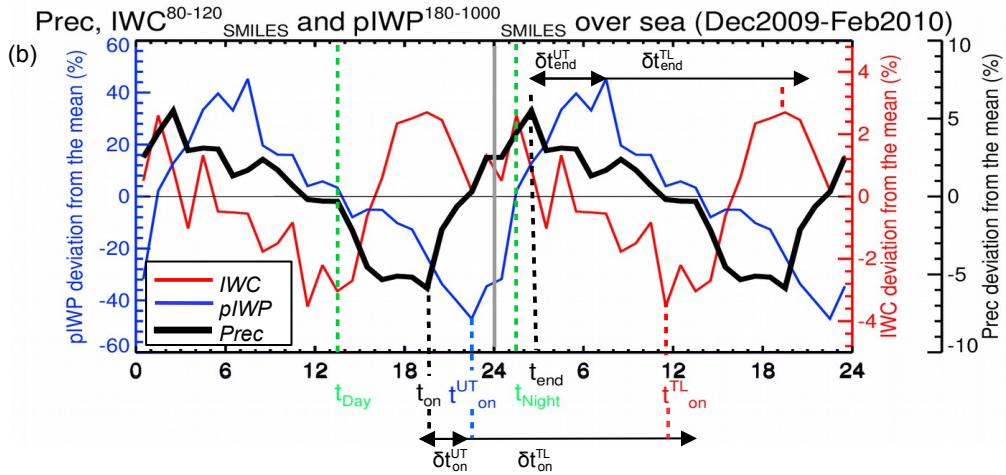
✕ representing the minimum of precipitation ( $Prec_{min}$ ) with its associated time ( $t_{on}$ ) and  $Prec$  during the day ( $Prec_{Day}$ ) at  $t_{Day} = 13:30$  LT. (b) Diurnal cycle of  $IWC^B(t)$  in red solid line, estimated from the diurnal cycle of  $Prec$  and from the two MLS measurements of ice (◇,  $IWC_x^B$ ), with the timing of the onset of the ice injection at  $t_{on}^B = t_{on} + \delta t^B$ . ■ represents the IWC maximum ( $IWC_{max}^B$ ) and □, the  $IWC_{min}^B$  when  $\delta t^B > 1h$ . Note that when  $t_{on} \approx t_{on}^B$ , the diurnal cycle of IWC is the red dashed line.

1095



1100

1105



1110

Figure 9: Deviation from the mean (%) of the diurnal cycle of partial Ice Water Path (pIWP, integrated between 1000 and 180 hPa), Ice Water Content (IWC, averaged between 80 and 120 hPa) measured by SMILES and precipitation (Prec) over (a) the tropical land (0°S-30°S) and (b) tropical ocean (0°N-30°S) from December 2009 to February 2010.  $t_{on}$ ,  $t_{on}^{UT}$  and  $t_{on}^{TL}$  are the onset of the Prec, pIWP and IWC increase, respectively.  $t_{end}$  is the end of the Prec increase.  $\delta t_{on}^{UT}$  and  $\delta t_{on}^{TL}$  are the delay between  $t_{on}$  and  $t_{on}^{UT}$  and  $t_{on}^{TL}$ , respectively and  $\delta t_{end}^{UT}$  and  $\delta t_{end}^{TL}$  are the delay between  $t_{end}$  and the end of the pIWP and IWC increase, respectively.

All the data have been filtered with a 6-h running average. Data have been smoothed out using 6-h running average.

**Table 1: Pearson linear correlation coefficient  $R$ , regression coefficient  $\alpha$  ( $\text{mg m}^{-3} \text{mm}^{-1} \text{h}$ ) and the offset  $\beta$  ( $\text{mg m}^{-3}$ ) from the correlation between precipitation and Ice Water Content (IWC), and Water Vapour (WV) in the upper troposphere (UT, at 146 hPa), at Day, Night and Day–Night over the 7 tropical zones and the average over the 6 zones ( $\mu_{6Zones}$ ).**

		Land			Ocean			MariCont	$\mu_{6Zones}$
		SouthAm	SouthAfr	MariCont-L	IndOc	PacOc	MariCont-O		
<b>IWC</b>	$R (IWC^{UT}_{Day}, P_{Day})$	0.7	0.8	0.5	0.8	0.8	0.6	0.5	0.7
	$\alpha (IWC^{UT}_{Day}, P_{Day})$	8.1	15	9.3	4.8	5.9	7.5	8.9	8.4
	$\beta (IWC^{UT}_{Day}, P_{Day})$	0.9	0.0	1.1	0.3	0.4	0.7	1.0	0.6
	$R (IWC^{UT}_{Night}, P_{Night})$	0.7	0.7	0.6	0.9	0.7	0.6	0.6	0.7
	$\alpha (IWC^{UT}_{Night}, P_{Night})$	4.8	6.1	5.6	4.7	6.8	7.7	5.4	5.9
	$\beta (IWC^{UT}_{Night}, P_{Night})$	0.6	0.6	1.4	0.3	0.2	0.6	1.6	0.6
	$R (IWC^{UT}_{Day-Night}, P_{Day-Night})$	0.6	0.7	0.7	0.1	0.2	0.5	0.5	0.5
<b>WV</b>	$R (WV^{UT}_{Day}, P_{Day})$	0.4	0.3	0.2	0.0	0.3	0.1	0.2	0.2
	$\alpha (WV^{UT}_{Day}, P_{Day})$	0.0	0.0	0.0	0.0	0.0	0.0	0.0	0.0
	$R (WV^{UT}_{Night}, P_{Night})$	0.5	0.5	0.1	0.0	0.5	0.0	0.0	0.3
	$\alpha (WV^{UT}_{Night}, P_{Night})$	0.0	0.0	0.0	0.0	0.0	0.0	0.0	0.0
	$R (WV^{UT}_{Day-Night}, P_{Day-Night})$	-0.0	-0.1	0.2	0.2	0.0	0.1	0.2	0.1

1135 **Table 2: Differences between the amount of Ice Water Content (IWC) estimated from TRMM and MLS injected in the upper troposphere (UT) and the tropopause layer (TL) ( $\Delta IWC^{UT}$  and  $\Delta IWC^{TL}$ , respectively), and partial Ice Water Path (pIWP) measured by SMILES in the UT ( $\Delta pIWP_{SMILES}$ ) and IWC measured by SMILES in the TL ( $\Delta IWC_{SMILES}$ ), during the period DJF 2009-2010, and their differences ( $\Delta IWC^{UT}-\Delta pIWP_{SMILES}$  and  $\Delta IWC^{TL}-\Delta IWC_{SMILES}$ , in the UT and the TL, respectively). The average over the land and ocean zones ( $\mu(Lands\ ZonesTropics)$ ,  $\mu(Oceans\ ZonesTropics)$ , respectively) are also presented.**

		UT			TL		
		$\Delta IWC^{UT}$ ( $mg\ m^{-3}$ )	$\Delta pIWP_{SMILES}$ ( $mg\ m^{-3}$ )	$\Delta IWC^{UT}-$ $\Delta pIWP_{SMILES}$ ( $mg\ m^{-3}$ )	$\Delta IWC^{TL}$ ( $mg\ m^{-3}$ )	$\Delta IWC_{SMILES}$ ( $mg\ m^{-3}$ )	$\Delta IWC^{TL}-$ $\Delta IWC_{SMILES}$ ( $mg\ m^{-3}$ )
L	SouthAm	2.13	2.85	-0.72	0.34	0.29	+0.05
A	SouthAfr	1.53	1.85	-0.32	0.23	0.27	-0.04
N	MariCont-L	2.52	2.33	+0.192	0.35	0.23	+0.12
D							
O	IndOc	1.13	1.01	+0.12	0.34	0.09	+0.15
C	PacOc	1.05	1.566	-0.51	0.21	0.24	-0.03
E	MariCont-O	0.495	1.05	-0.566	0.10	0.08	+0.02
A							
N							
	$\mu(Lands\ ZonesTropics)$	2.061	2.34	-0.283	0.31	0.26	+0.05
	$\mu(Oceans\ ZonesTropics)$	1.22	1.20	+0.02	0.22	0.13	+0.09

1140

1145

1150 **Table 3: Time of the onset of the ice injection in the tropical upper troposphere (UT), ( $t_{on}^{UT}$ ), duration of the injection of ice in the UT ( $\Delta t^{UT}$ ), minimum amount of ice in the UT ( $IWC_{min}^{UT}$ ), and amount of ice injected into the UT ( $\Delta IWC^{UT}$ ) as a function of the 6 study zones and averaged over the land and ocean zones ( $\mu(Lands\ ZonesTropics)$ ,  $\mu(Oceans\ ZonesTropics)$ , respectively) during DJF from 2004 to 2017. The bolded values highlight the most important injection of ice and the associated regions.**

Region	$t_{on}^{UT}$ (LT)	$\Delta t^{UT}$ (h)	$IWC_{on}^{UT}$ (mg m <sup>-3</sup> )	$\Delta IWC^{UT}$ (mg m <sup>-3</sup> )
SouthAm	08:00-09:00	7	1.6 <del>5</del>	<b>2.0</b> <del>1.99</del>
SouthAfr	08:00-09:00	7	1.3 <del>3</del>	<b>2.9</b> <b>86</b>
<b>MariCont-L</b>	08:00-09:00	8	1.0 <del>4</del>	<b>3.3</b> <b>4</b>
IndOc	17:00-18:00	9	1.0 <del>1</del>	0.4 <del>3</del>
PacOc	17:00-18:00	9	<b>1.5</b> <b>46</b>	<b>0.5</b> <b>46</b>
<b>MariCont-O</b>	17:00-18:00	11	1.6 <del>2</del>	<b>0.9</b> <b>1</b>
$\mu(Lands\ ZonesTropics)$	08:00-09:00	7	1.3 <del>4</del>	2.7 <del>3</del>
$\mu(Oceans\ ZonesTropics)$	17:00-18:00	10	1.3 <del>6</del>	0.6 <del>0</del>

1155

1160

1165

1170 **Table 4:** As a function of the delay ( $\delta t = 0, 1, 2, \text{ or } 3 \text{ h}$ ) between the beginning of the Prec onset and the IWC onset in the tropical tropopause layer (TL): **time of the onset of the ice injection in the TL** ( $\delta t \rightarrow \delta t_{on}^{TL}$ ), **duration of the injection of ice in the TL** ( $\Delta t^{TL}$ ), **minimum amount of ice in the TL** ( $IWC_{min}^{TL}$ ) and **amount of ice injected into the TL** ( $\Delta IWC^{TL}$ ) as a function of the 6 study zones and averaged over the land and ocean zones ( $\mu(Lands\ ZonesTropics)$ ,  $\mu(Oceans\ ZonesTropics)$ , respectively) during DJF from 2004 to 2017. The bolded values highlight the most important  $IWC_{min}^{TL}$  and  $\Delta IWC^{TL}$  and the associated regions.

Zones	$\delta t = 0 \text{ h}$			$\delta t = 1 \text{ h}$			$\delta t = 2 \text{ h}$			$\delta t = 3 \text{ h}$		
	$\Delta t^{TL}$ (h)	$IWC_{min}^{TL}$ ( $\text{mg m}^{-3}$ )	$\Delta IWC^{TL}$ ( $\text{mg m}^{-3}$ )	$\Delta t^{TL}$ (h)	$IWC_{min}^{TL}$ ( $\text{mg m}^{-3}$ )	$\Delta IWC^{TL}$ ( $\text{mg m}^{-3}$ )	$\Delta t^{TL}$ (h)	$IWC_{min}^{TL}$ ( $\text{mg m}^{-3}$ )	$\Delta IWC^{TL}$ ( $\text{mg m}^{-3}$ )	$\Delta t^{TL}$ (h)	$IWC_{min}^{TL}$ ( $\text{mg m}^{-3}$ )	$\Delta IWC^{TL}$ ( $\text{mg m}^{-3}$ )
SouthAm	7	0.22	0.26	6	0.23	0.25	5	0.28	0.20	4	0.35	0.13
SouthAfr	7	0.19	0.40	6	0.21	0.38	5	0.26	0.33	4	0.35	0.24
<b>MariCont-L</b>	8	0.17	<b>0.56</b>	7	0.19	<b>0.55</b>	6	0.23	<b>0.50</b>	5	0.32	<b>0.42</b>
IndOc	9	0.24	0.10	8	0.24	0.10	7	0.25	0.09	6	0.26	0.09
PacOc	9	0.29	0.09	8	0.29	0.09	7	0.29	0.09	6	0.30	0.08
<b>MariCont-O</b>	11	<b>0.34</b>	<b>0.19</b>	10	<b>0.35</b>	<b>0.18</b>	9	<b>0.36</b>	<b>0.17</b>	8	<b>0.37</b>	<b>0.16</b>
$\mu(Lands\ ZonesTropics)$	7	0.19	0.41	6	0.21	0.39	5	0.26	0.34	4	0.34	0.26
$\mu(Oceans\ ZonesTropics)$	10	0.29	0.13	9	0.29	0.12	8	0.30	0.12	7	0.31	0.11

1175

1180

1185 **Table 5: Difference  $d$  between Ice Water Content measured by MLS during the decreasing phase ( $IWC_x$ ) and Ice Water Content estimated at the same hour ( $IWC(x)$ ) in the upper troposphere (UT) and the tropopause layer (TL), (where  $x$  = Day or Night as a function of the timing of the decreasing phase of the ice diurnal cycle).**

Zones		$d$ in the UT (%)	$d$ in the TL (%)
		$d$ in the UT (mg.m <sup>-3</sup> )	$d$ in the TL (mg.m <sup>-3</sup> )
L A N	SouthAm	+0.48 (+ 23 %)	-0.08 (- 20 %)
	SouthAfr	+0.44 (+ 20 %)	-0.07 (- 18 %)
D	MariCont-L	-0.09 (- 3 %)	-0.09 (- 14 %)
O C E	IndOc	0.17 (- 21%)	-0.02 (- 7 %)
	PacOc	-0.20 (- 10 %)	+0.03 (+ 9 %)
A N	MariCont-O	-0.47 (- 26 %)	-0.04 (- 8 %)

1190

1195

1200

## Appendix 1: List of Abbreviations and Acronyms and Their Meanings

1205

<b>Acronyms</b>	<b>Meanings</b>
CPT	Cold Point Tropopause
DJF	December, January, February
IndOc	Indian Ocean
IWC	Ice Water Content
LS	Lower Stratosphere
LT	Local Time
MariCont	Maritime Continent
MariCont-L	Maritime Continent land
MariCont-O	Maritime Continent ocean
MLS	Microwave Limb Sounder
Prec	Precipitation
pIWP	partial Ice Water Path
PacOc	Pacific Ocean
RHI	Relative Humidity with respect to Ice
SouthAm	South America
SouthAfr	South Africa
TEMP	Temperature
TL	Tropopause Layer
TRMM	Tropical Rain Measuring Mission
TST	Troposphere to Stratosphere Transport
TTL	Tropical Tropopause Layer
UT	Upper Troposphere
WV	Water Vapour

1210